

Miocene basement exhumation in the Central Alps recorded by detrital garnet geochemistry in foreland basin deposits

Laura Stutenbecker^{1*}, Peter M.E. Tollan², Andrea Madella³, Pierre Lanari²

¹*Institute of Applied Geosciences, Technische Universität Darmstadt, Schnittspahnstr. 9, 64287 Darmstadt, Germany*

²*Institute of Geological Sciences, University of Bern, Baltzerstrasse 1+3, 3012 Bern, Switzerland*

³*Department of Geosciences, University of Tuebingen, Wilhelmstr. 56, 72074 Tuebingen, Germany*

*corresponding author: stutenbecker@geo.tu-darmstadt.de

Abstract

The Neogene evolution of the European Alps was characterized by the exhumation of crystalline basement, the so-called external crystalline massifs. Their exhumation presumably controlled the evolution of relief, distribution of drainage networks and generation of sediment in the Central Alps. However, due to the absence of suitable proxies, the timing of their surficial exposure, and thus the initiation of sediment supply from these areas, are poorly constrained.

The northern Alpine foreland basin preserves the Oligocene to Miocene sedimentary record of tectonic and climatic adjustments in the hinterland. This contribution analyses the provenance of 25 to 14 My-old alluvial fan deposits by means of detrital garnet chemistry. Unusually grossular- and spessartine-rich garnets ~~is~~^{are} found ~~to be~~^{(1) to be a} unique proxy^{ies} for identifying detritus from the external crystalline massifs and (2) to occur abundantly in ca. 14 My-old deposits of the. ~~In the foreland basin, these this garnets are is abundant in 14 My-old deposits. In contrast to previous assumptions, we therefore propose that the external massifs were already exposed to the surface ca. 14 My ago, thus providing a minimum age for the surficial exposure of the crystalline basement.~~

1. Introduction

Tectonic processes ~~influence-drive~~ the evolution of relief in mountain chains and consequently control the development of the drainage network, sediment supply and deposition in the foreland basin. The Central European Alps and their northern foreland basin, formed through the collision of the European and the Adriatic continents since the Eocene (Schmid et al. 1996; Handy et al. 2010), are a classic example of such interactions (e.g. Schlunegger et al., 1998; Pfiffner et al., 2002; Vernon et al., 2008, 2009; Baran et al., 2014; Fox et al., 2015). The exhumation of large slices of mid-crustal rocks from the European plate, the so-called external crystalline massifs, occurred ~~during a late-stage orogenic event~~ relatively late in the Alpine evolution, probably during the late Miocene, although the exact timing is not well constrained. The external crystalline massifs are today characterized by high relief, intense glaciation and some of the highest denudation rates ~~measured in the Alps (up to 1.4 mm/y), which all contribute to their importance~~ as a sediment source (Kühni and Pfiffner, 2001; Wittmann et al., 2007; Stutenbecker et al., 2018). The exhumation is discussed to be related to ~~possibly controlled by~~ crustal delamination in response to lithospheric mantle rollback (Herwegh et al., 2017), slab detachment (Fox et al., 2015) or erosional unloading (Champagnac et al., 2009), possibly due to increased precipitation rates in the Pliocene (Cederbom et al., 2004) or enhanced glacial erosion in the Pleistocene (Fox et al., 2015; Herman et al., 2013). ~~The areas exhumed during this event are today characterized by high relief, intense glaciation and some of the highest denudation rates measured in the Alps (up to 1.4 mm/y), which all contribute to their importance as a sediment source (Kühni and Pfiffner, 2001; Wittmann et al., 2007; Stutenbecker et al., 2018).~~

Peak metamorphism of lower to upper greenschist-facies conditions occurred between 17 and 22 Ma in all northern external crystalline massifs (Mont Blanc, Aar massifs and the Gotthard nappe, Challandes et al., 2008; Rolland et al., 2008; Cenki-Tok et al., 2014; Nibourel et al., 2018). Their subsequent exhumation has been investigated using thermochronology ~~by a number of studies~~ (e.g. Schaer et al., 1975; Wagner et al., 1977; Michalski and Soom, 1990; Vernon et al., 2009; Glotzbach et al., 2010). ~~While-Whereas~~ some studies concluded that exhumation was episodic (e.g. Vernon et al., 2009), others suggest relatively constant exhumation rates of 0.5-0.7 km/My since 14 My (Michalski and Soom, 1990; Glotzbach et al., 2010). A focus in this debate concerns the late Neogene cooling and the onset of glaciation in the Pleistocene and their possible effect on the exhumation, erosion and sediment accumulation rates (e.g. Kuhlemann et al., 2002; Herman et al., 2013; Schildgen et al., 2017). In contrast, the ~~Paleogene and early Neogene exhumation history is received comparably little attention less well studied~~. In particular, ~~the timing of the first surficial exposure of the external massifs has, however, for example, has~~ never been constrained, because estimates of their total thickness have not ~~yet been established yet~~. In most geometric reconstructions (e.g. Pfiffner, 1986; Pfiffner, 2017; Schmid et al., 2004), the contact between the crystalline basement and the overlying Mesozoic cover is assumed to be relatively flat, and the top of the crystalline basement is hypothesized to have been less than one kilometer above the modern topography. Conversely, a new reconstruction of this tectonic contact allows for a substantially greater amount (~8 km) of (now eroded) crystalline rock on top of the present-day topography (Nibourel et al., 2018).

This study aims to constrain the timing of exposure, and thus the beginning of sediment supply from the external crystalline massifs, by determining the provenance of the foreland basin deposits. Sedimentary rockss preserved in the northern peripheral foreland basin of the Central Alps, the Swiss part of the Molasse basin, are a well-studied archive recording tectonic and climatic adjustments in the central orogen between ca. 32 and 14 My ago (Schlunegger et al., 1993, 1996; Kempf et al., 1999; Spiegel et al., 2000; Kuhlemann and Kempf, 2002; von Eynatten, 2003; Schlunegger and Kissling, 2015). So far, the provenance of the Molasse deposits has been investigated using optical heavy mineral analysis, framework petrography and both bulk and single-grain geochemical techniques,

including epidote geochemistry and cooling ages derived from zircon fission track analysis and Ar-Ar dating of white mica (Spiegel et al., 2000, 2002; von Eynatten, 2003; von Eynatten and Wijbrans, 2003). No conclusive evidence for a contribution from the external crystalline massifs, however, has remained been found thus far elusive, leading to the assumption that their exposure must post-date the youngest preserved (ca. 14 My-old) Molasse sediments-deposits (von Eynatten, 2003).

In this study, we use detrital-garnet-major element geochemistry of detrital garnet in Miocene deposits preserved-infrom the central part of the Swiss foreland basin. The great compositional variability displayed by garnet from different source rocks means that it is a useful provenance tracer in a variety of settings (Spear, 1994; Mange and Morton, 2007). Furthermore, it is a common heavy mineral in (orogenic) sediments and sedimentary rocks (Garzanti and Andò, 2007) and is relatively stable during transport and diagenesis (Morton and Hallsworth, 2007). In the Central Alps, detrital garnet has recently been shown to be a valuable provenance indicator, especially for distinguishing detritus supplied from the external crystalline massifs (Stutenbecker et al., 2017). We aim (1) to explore if detrital garnet geochemistry can help identifying additional provenance changes in the Miocene Molasse deposits that have gone unnoticed so far provide additional provenance information to unravel the Miocene history of the Molasse deposits and its tectonic forcing and (2) to test whether detritus from the external massifs is present in the younger Molasse deposits in order to give independent constraints on the timing of crystalline basement exhumation.

1.1 Geological Setting

The Central Alps evolved through convergence between the European continental margin in the north and the Adriatic plate in the south (Schmid et al., 1996). The convergence started in-during the late Cretaceous with the subduction of the Alpine Tethys Ocean below the Adriatic microplate (Froitzheim et al., 1996), and ceased in-during the Paleogene after the European continental lithosphere entered the subduction zone. These Cretaceous to early Neogene orogenic processes are reflected by the syn-orogenic deposition of deep-marine flysch units preserved throughout the Alps (see e.g. Wildi, 1985; Winkler, 1996). Around 32 Ma ago, the sedimentation style in the northern foreland basin changed from marine, flysch-like deposition to shallow marine and terrestrial sedimentation (Allen et al., 1991; Sinclair, 1997). This is thought to represent the transition to Molasse-type sedimentation in an overfilled basin and is discussed to be potentially related to a breakoff of the European slab around the time of the Eocene-Oligocene boundary (e.g. Sinclair et al., 1991; Sinclair, 1997; Schlunegger and Kissling, 2015). Since this time, the northern foreland basin has become a major sink of orogenic detritus and an important sedimentary archive.

The sedimentary rocks in the Swiss part of the northern foreland basin are divided into four lithostratigraphic units that represent two shallowing- and coarsening-up megacycles (Schlunegger et al., 1998). The first cycle consists of the Rupelian Lower Marine Molasse (LMM) and the Chattian and Aquitanian Lower Freshwater Molasse (LFM). The second megacycle comprises a transgressive facies of Burdigalian age (the Upper Marine Molasse, UMM) overlain by Langhian to Serravalian deposits of the Upper Freshwater Molasse (UFM). The depositional ages of these units were constrained using mammal biostratigraphy and magnetostratigraphy (Engesser, 1990; Schlunegger et al., 1996). Throughout the Oligocene and the Miocene, the proximal Molasse deposits are thought to have been formed through a series of large alluvial fans (Fig. 1) aligned along the Alpine thrust front (Schlunegger et al., 1993; Kuhlemann and Kempf, 2002). The more distal parts of the basin were instead characterized by axial drainage directed towards the Paratethys in the East/Northeast (31-20 My) and the Western-western Mediterranean Sea in the Southwest-southwest (after 20 My), respectively (Kuhlemann and Kempf, 2002). Whereas the more distal deposits could be significantly influenced by long-distance transport from the northeast or southwest, the alluvial fans

are thought to carry a local provenance signal from the rocks exposed immediately south of each fan system due to their proximal nature.

The hinterland of the central Swiss foreland basin comprises, from north to south, potential source rocks derived from the following ~~architectural elements~~ tectonic units (Figs. 1, 2):

- (1) The Prealps Romandes; a stack of non-metamorphic and weakly metamorphosed sedimentary cover nappes (Mesozoic carbonates and Cretaceous-Eocene flysch), interpreted as the accretionary wedge of the Alpine Tethys, detached from its basement and thrust northwards onto the European units.
- (2) The Helvetic nappes; the non- or very low-grade metamorphic sedimentary cover sequence of the European continental margin (mostly Mesozoic carbonates).
- (3) The external crystalline massifs; lentoid-shaped autochthonous bodies of European continental crust that consist of a pre-Variscan polycyclic gneiss basement intruded by Upper Carboniferous to Permian granitoid rocks and an overlying metasedimentary cover. They were buried within the Alpine nappe stack ~~in~~ during the Oligocene (Cenki-Tok et al., 2014), reaching greenschist facies peak-metamorphic conditions between 17 and 22 My ago (Fig. 2a) and were exhumed during the Miocene. The Gotthard nappe, although not a “massif” *sensu stricto* because of its allochthonous nature, will be included ~~into~~ the term “external crystalline massifs” from here on, because the timing and the rates of exhumation are comparable (Fig. 2b, Glotzbach et al., 2010).
- (4) The Lepontine dome; an allochthonous nappe stack of European Paleozoic gneiss basement and its Mesozoic metasedimentary cover (Berger et al., 2005). Amphibolite-facies peak metamorphism (Frey and Ferreiro Mählmann 1999; Fig. 2a) in the Lepontine occurred diachronously at around 30-27 My ago in the south (Gebauer, 1999) and possibly as late as 19 My ago in the north (Janots et al., 2009). Although the onset of exhumation of the Lepontine dome might have been equally diachronous, it is generally assumed to have occurred before 23 My ago (Hurford, 1986).
- (5) The Penninic nappes, containing ophiolites of the Alpine Tethys as well as the continental crust of Briançonnais, a microcontinent located within the ~~a~~ Alpine Tethys between the southern Piedmont-Ligurian ocean and the northern Valais trough (Schmid et al., 2004).
- (6) The Austroalpine nappes, containing the basement and sedimentary cover of the Adriatic plate with a Cretaceous (“Eoalpine”, ca. 90-110 My) metamorphic peak of greenschist facies conditions (Schmid et al., 2004). ~~Although the~~ The Austroalpine nappes were probably part of the nappe stack in the Central Alps prior to their erosion during the Oligocene and Miocene although they are found exclusively in the Eastern Alps to the east of the Lepontine dome today; ~~we mention them here as well, because they were probably part of the nappe stack in the Central Alps prior to their erosion during the Oligocene and Miocene.~~
- (7) The Sesia/Dent Blanche nappe, probably representing rifted segments of the basement and sedimentary cover of a distal part of the Adriatic plate (Froitzheim et al., 1996). In contrast to the Austroalpine nappes, the Sesia/Dent Blanche nappe was subducted and exposed to blueschist-facies (Fig. 2a; Bousquet et al., 2012; Fig. 2) to eclogite-facies metamorphism (e.g. Oberhänsli et al., 2004).

1.2 Compositional trends in the Honegg-Napf fan

~~Rocks from the~~ The Central Alps are generally considered as the major sediment source of all proximal Molasse basin deposits, ~~while and~~ compositional changes in the foreland are thought to directly reflect tectonic and erosional processes in the immediate Alpine hinterland (Matter, 1964; Schlunegger et

al., 1993; 1998). The compositional evolution in the basin is diachronous and ~~not~~-uniform between the different fan systems (e.g. Schlunegger et al., 1998; Spiegel et al., 2000; von Eynatten, 2003). In this study, we will focus on the Honegg-Napf fan, located in the central part of the basin. ~~It which is the most likely to archive~~preserves a provenance signal related to external massif exhumation due to its proximity to the large crystalline basement slices of the Aar massif and the Gotthard nappe (Fig. 1). In the Honegg-Napf fan, three major compositional trends have been previously identified (Fig. 3):

(Phase 1) Between ~31 and ~25 My ago, the heavy minerals are dominated by the zircon-tourmaline-rutile (~~ZTR~~)-assemblage and garnet (von Eynatten, 2003). Rock fragments are dominantly of sedimentary origin and zircon fission track ages are Paleozoic to late Mesozoic (Spiegel et al., 2000). This phase is consistently interpreted ~~by different authors~~ to reflect the erosion of ~~(Austroalpine)~~ flysch-like sedimentary cover nappes, which are structurally the highest top in of the central ~~a~~Alpine nappe stack and probably extended further west during this time (Schlunegger et al., 1998; Spiegel et al., 2000; von Eynatten, 2003).

(Phase 2) 25-21 My ago: Around 25 My ago, the occurrence of epidote as well as an increase in ~~granitic-granitoid~~ rock fragments mark a major compositional change in the foreland. The presence of characteristic colorful granite pebbles suggests an origin from the Austroalpine Bernina nappe (Matter, 1964). Sediments of this phase clearly reflect the ~~down-cutting~~ down into crystalline basement and are consistent with a continuation of a normal unroofing sequence. Additionally, ~~(Schlunegger et al., 1998)~~ report the occurrence of quartzite pebbles, possibly sourced from the middle Penninic Siviez-Mischabel nappe and argue that parts of the epidote could originate from Penninic ophiolites as well, thus suggesting that erosion might have ~~already~~-reached down into the Penninic nappes already by then. Spiegel et al., (2002) argued against this Penninic contribution based on the $^{87}\text{Sr}/^{86}\text{Sr}$ and $^{143}\text{Nd}/^{144}\text{Nd}$ isotopic signatures of the epidote.

(Phase 3) 21-14 My ago: At ~21 My, metamorphic rock fragments occur in the sediments, ~~while~~ whereas the heavy mineral assemblages remain epidote-dominated and overall similar to the second phase. Zircon fission track ages are exclusively Cenozoic (ages peak between ~32 and ~19 Ma). In contrast to the first two phases, the sediment composition allows several, partially contradicting interpretations. Whilst petrographical and mineralogical data might suggest recycling and sediment mixing (von Eynatten, 2003), young $^{40}\text{Ar}/^{39}\text{Ar}$ cooling ages in white mica (von Eynatten, 2003; von Eynatten and Wijbrans, 2003) and ~~exclusively young a population of zircons with a~~ fission track central ages of 19.5±0.9 My-(Spiegel et al., 2000) point to an additional, newly exhumed source ~~that these authors identified~~ as the Lepontine dome (Fig. 2b; von Eynatten, 2003; Spiegel et al., 2000). Based on the abundance of flysch pebbles after ~21 My, Schlunegger et al. (1998) favor an alternative scenario, in which the erosional front shifted northwards into the flysch nappes of the Prealps Romandes. A mixture of both sources seems possible. Furthermore, the isotopic signature of detrital epidotes suggests a contribution of mantle source rocks between ca. 21 and 19 My ago, which could point to a contribution by Penninic ophiolites (Spiegel et al., 2002). However, this is not reflected in the heavy mineral spectra (von Eynatten, 2003) ~~that, which~~ do not contain typical ophiolite minerals such as Cr-spinel.

~~In none of these scenarios were~~ The external crystalline massifs have not been considered as a possible sediment source. The exact time of their surficial exposure is unknown, but it is believed to post-date the youngest preserved Molasse sediments/deposits. This interpretation is based on the lack of granitic pebbles attributable to the external massifs in the Molasse (Trümpy, 1980) and on structural reconstructions (e.g. Pfiffner, 1986) in combination with thermochronological data (e.g. Michalski and Soom, 1990).

2. Sampling strategy and methodology

In order to characterize the detrital garnets in the foreland, three samples were taken from 25 My-, 19 My- and 14 My-old fine- to medium-grained fluvial sandstones within the Honegg-Napf fan deposits located ca. 40 kilometers to the East-east and Southeast-southeast of Berne in the central part of the Swiss Molasse basin. The exact sampling sites were chosen based on the availability of published petrographical, chemical and mineralogical data (von Eynatten, 2003) as well as magnetostratigraphic calibration (Schlunegger et al., 1996).

It is possible to compare potential source compositions to the detrital ones, ~~b~~Because the potential source rocks were already narrowed down to particular regions based on other provenance proxies, and because many of these rocks are still preserved in the Alpine chain today, ~~it is possible to compare potential source compositions to the detrital ones.~~ For comparison we used detrital data from Stutenbecker et al. (2017) as well as published source rock data from different units across the Central Alps (Steck and Burri, 1971; Chinner and Dixon, 1973; Ernst and Dal Piaz, 1978; Hunziker and Zingg, 1980; Oberhänsli, 1980; Sartori, 1990; Thélin et al., 1990; Reinecke, 1998; von Raumer et al., 1999; Cartwright and Barnicoat, 2002; Bucher and Bousquet, 2007; Angiboust et al., 2009; Bucher and Grapes, 2009; Weber and Bucher, 2015).

In addition, three river sand samples were collected from small monolithological catchments (3-30 km²) draining potentially garnet-bearing ~~potential~~ source rocks that were previously not, or only partially, considered in the literature. We prefer this “tributary sampling approach” (first-order sampling scale according to see e.g. Stutenbecker et al., 2017Ingersoll, 1990) over in-situ sampling of specific source rocks, because small monolithological catchments are more likely to comprise all garnet varieties of the targeted source rock and to average out spatial variations of the source rock properties, e.g. mineral size or fertility (Malusà et al., 2016). ~~differences in garnet fertility.~~ The targeted plausible source areas are located ~~within-in~~ the Gurnigel flysch (Prealpes Romandes), the Antigorio nappe orthogneisses of the Lepontine dome, and the Lebendun nappe paragneisses of the Lepontine dome (Fig.1). Sample characteristics are summarized in Table 1 and Table 2. For detailed lithological descriptions of the ~~sampled-sampling~~ sites in the Honegg-Napf area, see Schlunegger et al. (1993) and von Eynatten (2003).

The sandstone samples were carefully disintegrated using a jaw breaker and a pestle and mortar. The disintegrated sandstones ~~as well as and~~ the source rock tributary sands were sieved into four grain size classes of <63 µm, 63-125 µm, 125-250 µm and >250 µm. The fractions of 63-125 µm and 125-250 µm were further processed in sodium polytungstate heavy liquid at 2.85 g/cm³ to concentrate heavy minerals. The heavy mineral concentrates were dried and, depending on the obtained amounts, split into 2-4 parts using a microsplitter. All ~~measured-analysed~~ garnet grains were hand-picked from the concentrate of one split part per fraction under a binocular microscope.

The grains were subsequently arranged in lines on sticky tape, embedded ~~into-in~~ epoxy resin, ground with SiC abrasive paper (grits 400, 800, 1200, 2500, 4000), polished using 3, 1 and ¼ µm diamond suspensions and graphite-coated. Major element oxides were analyzed using a JEOL JXA-8200 electron probe micro-analyzer at the Institute of Geological Science at University of Bern, Switzerland, under standard operating conditions for garnet (see Giuntoli et al., 2018): accelerating voltage of 15 kKeV, electron beam current of 15 nA, beam diameter of 1µm, 20 s peak acquisition time for Si, Ti, Al, Fe, Mn, Mg, Ca and 10 s for both backgrounds. Natural and synthetic standard olivine (SiO₂, MgO, FeO), anorthite (Al₂O₃, CaO) ilmenite (TiO₂) and tephroite (MnO) were used for calibration by applying a CITIZAF correction (Armstrong, 1984). Garnet compositions were measured as close as possible to the geometric centers of the grains, unless the area was heavily fractured or showed inclusions of other minerals. In some randomly selected grains core and rim compositions

were measured to identify intra-grain chemical variability; these core/rim pairs are reported separately in Stutenbecker (2019).

Molecular proportions were calculated from the measured main oxide compositions on the base of 12 anhydrous oxygen atoms. ~~Because ferric and ferrous iron were not measured separately ($\text{FeO} = \text{Fe}_{\text{total}}$),~~ The $\text{Fe}^{2+}/\text{Fe}^{3+}$ ratio was determined based on charge balance (Locock, 2008). ~~because ferric and ferrous iron were not measured separately ($\text{FeO} = \text{Fe}_{\text{total}}$).~~ Garnet endmember compositions were subsequently calculated using the Excel spreadsheet by Locock (2008). ~~Garnet is a solid solution between different endmembers, the most common ones being almandine ($\text{Fe}_3\text{Al}_2\text{Si}_3\text{O}_{12}$), grossular ($\text{Ca}_3\text{Al}_2\text{Si}_3\text{O}_{12}$), pyrope ($\text{Mg}_3\text{Al}_2\text{Si}_3\text{O}_{12}$), spessartine ($\text{Mn}_3\text{Al}_2\text{Si}_3\text{O}_{12}$) and andradite ($\text{Ca}_3\text{Fe}_2\text{Si}_3\text{O}_{12}$).~~ The relative proportions of these endmember components almandine ($\text{Fe}_3\text{Al}_2\text{Si}_3\text{O}_{12}$), grossular ($\text{Ca}_3\text{Al}_2\text{Si}_3\text{O}_{12}$), pyrope ($\text{Mg}_3\text{Al}_2\text{Si}_3\text{O}_{12}$), spessartine ($\text{Mn}_3\text{Al}_2\text{Si}_3\text{O}_{12}$) and andradite ($\text{Ca}_3\text{Fe}_2\text{Si}_3\text{O}_{12}$) depend on bulk rock composition and intensive parameters (such as temperature and pressure), which can vary substantially depending on the metamorphic or magmatic history of the protolith (Deer et al., 1992; Spear, 1994). The data were plotted and classified using the ternary diagram of Mange and Morton (2007) as well as the linear discriminant function method of Tolosana-Delgado et al. (2018) based on a global data compilation on garnet compositions from different source rocks (Krippner et al., 2014).

3. Results

Most of the detrital garnets are dominated by ~~the~~ Fe-rich almandine ~~endmember~~ with varying amounts of grossular, pyrope, spessartine and andradite (Fig. 4). Other endmembers (e.g. uvarovite) are negligible. ~~Minimum, maximum and average~~ Average endmember contents are summarized in Table 3; for the full dataset we refer to Stutenbecker (2019). Garnet compositions do not differ significantly between the two analyzed grain size fractions of the same sample, although ~~some~~ slight variations are visible ~~in the ternary plot~~ (Fig. 4): ~~in~~ In sample LS2016-18 (25 My, Fig. 4a) garnets of the 125-250 μm fraction ~~tend to be more~~ enriched in pyrope ~~with respect to~~ than garnets of the 63-125 μm fraction. In sample LS2018-5 (19 My, Fig. 4b) 4 “outliers” that are very pyrope- and grossular-rich ($n=2$) or grossular- and andradite-rich ($n=2$) occur only in the 63-125 μm grain size fraction. Furthermore, garnet grains of the 63-125 μm fraction are more frequently grossular-rich compared to the 125-250 μm fraction. In sample LS2017-3 (14 My, Fig. 4c), the 63-125 μm fraction contains some garnet grains ($n=8$) of high almandine and low grossular content that are absent in the 125-250 μm fraction.

Although some individual garnet ~~grainss~~ show distinct internal compositional zoning from core to rim, the intra-grain chemical variability is generally negligible (see Stutenbecker, 2019).

~~According to the ternary classification plot of Mange and Morton (2007),~~ ~~the~~ The major part of garnet in all three samples (>80 %) belong to the B-type garnet of Mange and Morton (2007) and thus point to a dominant contribution by amphibolite-facies source rocks (Table 4). Minor ~~portions-amounts~~ are ~~derived from~~ classified as C-type (high-grade metabasic), A-type (granulite facies) and D-type (metasomatic) ~~sources~~ garnet. The 25 My-old sandstone contains almost exclusively B-type garnet (92%, Table 4). The 19 My-old sandstone shows a larger spread with some A-, C- and D-type garnet (Fig. 4b, Table 4). The 14 My-old sandstone contains B-, C- and D-type garnet (Fig. 4c, Table 4). Classification through linear discriminant analysis (Tolosana-Delgado et al., 2018) yields a similar trend with generally high proportions of amphibolite-facies source rocks (class B-garnets, >70 %, Table 4). Some grains (5 %, 3 % and 12 % in the 25 My-, 19 My- and 14 My-old ~~samples~~ deposits, respectively) were classified as igneous garnet (Table 4).

Distinct compositional changes between the 25 My-, 19 My- and 14 My-old Molasse ~~sediments~~ ~~sandstones~~ are mostly related to the ratio of almandine and grossular contents (Table 3, Fig. 5). At 25 My, ~~the~~ garnets are dominantly almandine-rich (average 70 %) and grossular-poor (average 9 %). At 19 My, both grossular-poor and grossular-richer garnets occur (average 16 %). Garnets in the 14 My-old ~~sample sandstone~~ are generally almandine-poorer (average 50 %) and grossular-rich (average 32 %). ~~This implies (1) that garnets contained in the younger sediment (14 and, to some extent, 19 My) were not recycled in significant amounts from the older Molasse strata and (2) that at least two sources supplied B-type garnets during Molasse deposition.~~

~~Garnet compositions from the three potential source rock samples analyzed in this study are shown in Fig. 4d (Lepontine paragneiss and Lepontine orthogneiss) and Fig. 4e (Gurnigel flysch). The average compositions are displayed in Fig. 6; for the full dataset we refer to Stutenbecker (2019). Likewise, average compositions of garnet from the literature (external massif granite garnets, eclogite facies garnets and granulite facies garnets) are displayed in Fig. 6.~~

~~All source rocks, except for the external crystalline massif granites, supply almandine-dominated (i.e. >50 % almandine component) garnet. The andradite content in all source rock garnets is very low, but they contain varying amounts of grossular, spessartine and pyrope. Garnets from the Lepontine gneisses (Table 3, Fig. 4d) are generally almandine-rich, but those in the paragneiss tend to be grossular-richer (22 %) compared to the ones in the orthogneiss (11 %). The Gurnigel flysch garnets (Fig. 4e) are almandine-rich with elevated pyrope contents (14 %). Garnets from the external crystalline massifs (Fig. 4f) are unusually rich in grossular (35 %) and spessartine (21 %), and the almandine content is much lower than in the other source rock garnets (34 %). Eclogite facies garnets have high grossular (23 %) and pyrope (16 %) contents (Fig. 4g). Granulite facies garnets (Fig. 4g) have on average the highest pyrope content of all source rock garnets (25 %).~~

4. Discussion

4.1 Origin of amphibolite-facies garnets Late Oligocene (~25 My ago)

Although detrital garnet chemistry suggests the presence of only one relatively uniform, amphibolite-facies source rock in the hinterland of the Honegg-Napf fan during the late Oligocene, the identification of the exact nature of this source is difficult. This is mostly due to the large compositional overlap of garnet sourced by diverse amphibolite-facies metamorphic rocks (e.g. meta-sedimentary versus meta-igneous; Krippner et al., 2014; Tolosana-Delgado et al., 2018).

Amphibolite-facies conditions of Alpine age were only reached in the Lepontine dome (Fig. 2a; Bousquet et al., 2012). However, many gneisses in the Central Alps preserve a pre-Alpine amphibolite-facies metamorphic signature as well (Frey et al., 1999), for example in the Austroalpine Bernina nappe (Spillmann, 1993; Spillmann and Büchi, 1993), the middle Penninic Briançonnais basement (Sartori et al., 2006) or the polycyclic basement of the external massifs (von Raumer et al., 1999). In fact, the Gurnigel flysch, a Late Cretaceous to Eocene flysch nappe in the Prealps Romandes that did not undergo Alpine metamorphism (Fig. 2a), contains abundant almandine-rich B-type garnets (Fig. 4e).

Zircon fission track ages from sandstones of the same age are mostly >100 My old with a smaller and younger age peak of 41±9 My (Fig. 3; Spiegel et al., 2000). This would favor an input from the Austroalpine nappes and/or the Prealps Romandes (Fig. 67a), which yield related cooling ages >50 My (Fig. 2b; e.g. Bernet et al., 2009), rather than from the Lepontine dome, which is characterized by zircon fission track ages <30 My (Fig. 2b; e.g. Hurford, 1986). The presence of granite pebbles

attributable to the Austroalpine Bernina nappe (Matter, 1964; Schlunegger et al., 1998) would further support an Austroalpine rather than a Lepontine provenance. The drainage divide was probably located close to the Insubric line (e.g. Schlunegger et al., 1998), but north of the Bergell pluton (Fig. 67a), whose detritus is exclusively found in the retroforeland to the south (Gonfolite Lombarda; Giger and Hurford, 1989; Carrapa and Di Giulio, 2001). According to the compositional classification of Mange and Morton (2007) and Tolosana Delgado et al. (2018), the majority of detrital garnet grains in the Molasse were derived from amphibolite facies source rocks ("B-type"). Garnets derived from amphibolite facies rocks ("B-type") seem to be the most frequent ones in all three considered samples. In the Central Alps, amphibolite facies conditions of alpine age were only reached in the Lepontine nappes (Fig. 2). However, many gneisses in the area preserve a pre-Mesozoic amphibolite facies metamorphic signature as well (Frey et al., 1999), for example in the Austroalpine Bernina nappe (Spillmann, 1993; Spillmann and Büchi, 1993), the middle Penninic Briançonnais basement (Sartori et al., 2006) or the polycyclic basement of the external massifs (von Raumer et al., 1999). In fact, the Gurnigel flysch, a Late Cretaceous to Eocene flysch nappe in the Prealps Romandes that did not undergo alpine metamorphism (Fig. 2), contains almost exclusively almandine-rich B-type garnets (Fig. 4e). These considerations indicate that, following the classification scheme of Mange and Morton (2007) alone, the provenance of Alpine B-type garnets remains ambiguous. However, petrographic findings as well as zircon fission track analysis and Ar/Ar dating in white mica (Spiegel et al., 2000; von Eynatten, 2003; von Eynatten and Wijbrans, 2003) strongly suggest a compositional change ca. 21 My ago towards a metasedimentary source with a young cooling history. These authors relate this shift to the erosion of the sedimentary cover of the Lepontine dome. Source rock samples taken within the Lepontine dome from the crystalline basement (Antigorio nappe orthogneiss) and the meta-sedimentary cover (Lebendun nappe paragneiss) contain generally almandine-rich garnets, but those from the paragneiss tend to be richer in grossular than those from the orthogneisses (Fig. 4). Because the amount of grossular-rich garnet is higher in the 19 My old sample compared to the 25 My old sample, the data could support an origin from the Lepontine meta-sedimentary cover.

4.2 Origin of granulite-facies garnets Early Miocene (~19 My ago)

Granulite facies garnet grains with relatively high pyrope and low grossular contents ("A-type" and "Class C" garnets according to Mange and Morton (2007) and Tolosana Delgado et al. (2018), respectively) are only frequent in the 19 My old Molasse sample (ca. 8-9 %, Table 3).

The larger spread of garnet compositions in the early Miocene (~19 My) sample indicates the presence of several or mixed sources with different metamorphic grades, including amphibolite-, eclogite-, and granulite-facies rocks.

The B-type garnet compositions match the range of garnets found in the Lepontine nappes (Fig. 4b, d), which is supported by the occurrence of predominantly young (<30 My) zircon fission track ages (Fig. 3) that in agreement with match the the young cooling ages of the Lepontine dome (Fig. 2e; Bernet et al., 2009). Due to the overlap of amphibolite-facies garnets, it cannot be excluded Alpine that at least some of the garnets were contributed by Austroalpine sources or were recycled from older strata. The Lepontine dome was probably drained both towards the north and the south (Fig. 67b), because old basement detritus with young cooling ages (~30 My, derived from K-Ar on white mica) was found in the Gonfolite Lombarda group in the southern retroforeland (Giger and Hurford, 1989).

Granulite-facies metamorphic conditions in the Central Alps were only reached in the Gruf complex located close to the Insubric line between the Lepontine dome and the Bergell intrusion (Fig. 2a). Furthermore, there is evidence for pre-Mesozoic granulite-facies metamorphism in some rocks in the Southern Alpine Ivrea zone south of the Insubric line (Hunziker and Zingg, 1980), in the Sesia Zone (Fig. 1; Engi et al., 2018; Giuntoli et al., 2018) and in the Dent Blanche nappe (Fig. 1; Angiboust et

al., 2009). It is unlikely that erosion reached ~~so that~~ far to the South during the Miocene, because the Penninic and probably also the exhuming Lepontine nappe stack would have acted as a topographic barrier to the fluvial drainage network (Fig. 67b). However, it was proposed that the flysch ~~sediments~~ deposits preserved in the Prealps Romandes were partially fed by these units during the Late Cretaceous and the Eocene (Wildi, 1985; Ragusa et al., 2017). This interpretation is supported by the Gurnigel flysch sample (Fig. 4e), which contains garnet of granulite-facies type that are similar to those found in the Ivrea zone (Table 3, Fig. 4h). A recycled flysch origin is supported further by the abundance of flysch sandstone pebbles in Molasse strata of the same age (Schlunegger et al., 1998). A potential, but minor contribution from ophiolites, as suggested by Spiegel et al. (2002), could be supported by the two eclogite-facies garnet grains found in the 19 My-old sample (Fig. 4b) that match eclogite-facies garnets from Alpine ophiolites (Table 3, Fig. 4g). Eclogite-facies garnets ~~are known from~~ occur both metamorphic rocks of the Penninic Alpine ophiolites (e.g. Bucher and Grapes, 2009; Weber and Bucher, 2015, Fig. 2a), but also from Paleozoic (?) gneisses of the middle Penninic Briançonnais basement (Sartori, 1990; Thélin et al., 1990). Both sources are not distinguishable (Fig. 4g), but would have probably been located in relative close geographic proximity, either in the Penninic hanging wall south of the Simplon fault (Zermatt area) or in the Penninic nappes located between the eastern rim of the Lepontine and the adjacent Austroalpine nappes (Arosa zone; Fig. 76b).

4.3 ~~Origin of eclogite-facies garnets~~ Middle Miocene (~14 My ago)

Previous provenance studies have identified meta-sedimentary detritus in the Middle Miocene Molasse and located its source in the unroofing sedimentary cover of the Lepontine dome (e.g. von Eynatten, 2003). This was strongly supported by the ~~very~~ young detrital zircon fission track ages (youngest peak at 19.5 ± 0.9 My, Fig. 3; Spiegel et al., 2000) that match the zircon fission track ages of the Lepontine dome (Fig. 2b, e.g. Hurford, 1986; Berner et al., 2009).

However, garnet compositions in the youngest Molasse sandstones are not comparable to Lepontine garnets sampled in this study nor to any detrital garnet found in the main rivers draining the Lepontine dome today (Andò et al., 2014). Instead, the detrital garnet signature of the 14 My-old sample mirrors almost exactly the compositional range of garnets from the external crystalline massifs (Table 3, Fig. 4c, 4f). In the external crystalline massifs, these garnets grew in Permo-Carboniferous plutons under Alpine greenschist-facies metamorphic conditions (Steck and Burri, 1971, Fig. 2a). They are restricted to the granitoid basement of the external massifs and do not occur anywhere else in the Central Alps, which makes them an excellent provenance proxy (Stutenbecker et al., 2017). A further distinction among garnets supplied by the different plutons (e.g. the Central Aar granite from the Aar massif, the Rotondo granite from the Gotthard nappe and the Mont Blanc granite from the Mont Blanc massif) is not possible based on major element garnet geochemistry alone (Stutenbecker et al., 2017).

Until now, the surficial exposure of the external massifs in the Central Alps was thought to post-date Molasse deposition. This interpretation relies principally on the absence of pebbles of external massif origin (e.g. Aare granite) in the foreland basin (Trümpy, 1980). However, many Alpine granite bodies closely resemble each other mineralogically and texturally, especially if present as altered pebbles in the Molasse deposits, and hence it is difficult to discount a specific source only on this basis. Further support of late surficial exposure of the external massifs comes from structural reconstructions (e.g. Pfiffner, 1986; Pfiffner, 2017), that have located the top of the crystalline basement at an elevation that is similar to the modern topography, based on a relatively flat-lying contact between the crystalline basement and the overlying Mesozoic sedimentary cover (Fig. 78a). According to this model and the published exhumation rates of 0.5-0.7 km/My (Michalski and Soom, 1990; Glotzbach et al., 2010), the top of the basement was buried 7-10 km below the surface 14 Ma ago.

However, Nibourel et al. (2018) recently proposed a revised geometry of the contact between crystalline basement and overlying cover, which allows ca. 8 km of additional crystalline basement on

top of the present-day topography (Fig. 78b). The presence of external massif-sourced garnets in the youngest Molasse deposits provides independent evidence that parts of the crystalline crust comprised in the external massifs were already at the surface at ca. 14 Ma (Fig. 67c). Assuming the aforementioned average exhumation rates, 7-10 km of crystalline basement would have already been exhumed and subsequently eroded during the past 14 My, which is in good agreement with the geometric reconstructions by Nibourel et al. (2018).

We suggest that the drainage divide was shifted northwards due to the exhumation of the Gotthard nappe and/or the Aar massif and that it was essentially located at its current position (Fig. 67c, d), but this warrants corroboration from other deposits in the foreland and the retroforeland.

4.4 Origin of “igneous” garnets

Of the garnets from the youngest, 14 My old Molasse sample, 12 % can be classified as igneous (“Class E”, Table 4) according to Tolosana Delgado et al. (2018). Their high grossular and very low pyrope content distinguishes them clearly from all the other, generally more almandine rich, garnets. In the classification scheme after Mange and Morton (2007), however, this type of garnet plots in the D-type or in the rightmost part of the B-type or field (Fig. 4, Table 4). The detrital garnet signature of the 14 My old sample mirrors almost exactly the compositional range of garnets from the external crystalline massifs (Fig. 4c, 4f). In the external crystalline massifs, these garnets grew in Permo-Carboniferous plutons under alpine greenschist facies metamorphic conditions (Steck and Burri, 1971, Fig. 2). They are restricted to the granitoid basement of the external massifs and do not occur anywhere else in the Central Alps, which makes them an excellent provenance proxy (Stutenbecker et al., 2017). A further distinction among garnets supplied by the different plutons (e.g. the Central Aar granite from the Aar massif, the Rotondo granite from the Gotthard nappe or the Mont Blanc granite from the Mont Blanc massif) is not possible based on garnet major element geochemistry alone (Stutenbecker et al., 2017).

4.5 Implications for the evolution of the Alpine orogen

Previous provenance studies have identified meta-sedimentary detritus in the youngest (ca. 21-14 My old) Molasse and located its source in the unroofing sedimentary cover of the Lepontine dome (von Eynatten, 2003). This was strongly supported by the very young detrital zircon fission-track ages (youngest peak at 19.5 ± 0.9 My, Spiegel et al., 2000) that match the exhumation pattern zircon fission track ages of the Lepontine dome (e.g. Hurford, 1986; Bernet et al., 2009). However, garnet compositions in the youngest Molasse sandstones are not comparable to Lepontine garnets sampled in this study nor to any detrital garnet found in the main rivers draining the Lepontine dome today (Andò et al., 2014).

Instead, the occurrence of grossular- and spessartine-rich garnets in the 14 My old Molasse mark a distinct provenance change compared to the 19 My old deposits that was not noticed in previous studies (Schlunegger et al., 1998; Spiegel et al., 2000; von Eynatten, 2003). Garnets of this particular composition are described from the Permo-Carboniferous plutons intruded into the crystalline basement of the Aar and Mont Blanc massifs and the Gotthard nappe (Steck and Burri, 1971). Such particular chemical composition provides a unique sedimentary fingerprint (Stutenbecker et al., 2017). Their occurrence in the youngest Molasse sediments has important implications for the tectonic evolution of the orogen. Until now, the surficial exposure of the external massifs in the Central Alps was thought to post-date Molasse deposition. This interpretation relies principally on the absence of pebbles of external massif origin (e.g. Aare granite) in the foreland basin (Trümpy, 1980). However, many alpine granites closely resemble each other, especially if present as altered pebbles in the Molasse deposits, and hence it is difficult to discount a specific source only on this basis. Further support of late surficial exposure of the external massifs comes from structural reconstructions (e.g. Pfiffner, 1986; 2017), that have located the top of the crystalline basement similar to the modern

topography, based on a relatively flat lying contact between the crystalline basement and the overlying Mesozoic sedimentary cover (Fig. 7a). According to this model and the published exhumation rates of 0.5–0.7 km/My (Michalski and Soom, 1990; Glotzbach et al., 2010), the top of the basement must have been buried 7–10 km below the surface 14 Ma ago. However, Nibourel et al. (2018) have recently proposed a revised geometry of the contact between crystalline basement and overlying cover, which allows ca. 8 km of additional crystalline basement on top of the present-day topography (Fig. 7b). The presence of external-massif-sourced garnets in the youngest Molasse deposits provides independent evidence that parts of the crystalline crust comprised in the external massifs were already at the surface at ca. 14 Ma. Assuming the aforementioned average exhumation rates, 7–10 km of crystalline basement would have already been exhumed (and subsequently eroded) during the past 14 My, which is in good agreement with the geometric reconstructions by Nibourel et al. (2018).

The resulting implications for the paleogeography and drainage evolution of the Central Alps, and in particular for the direct hinterland of the Napf fan, are summarized in Fig. 8.

Although detrital garnet chemistry suggests exclusively contributions of amphibolite facies sources during the latest Oligocene (~25 My), this methodology cannot distinguish between the diverse amphibolite facies rocks present in the Central Alps (e.g. alpine metamorphic rocks in the Lepontine nappes vs. Paleozoic metamorphic rocks in the Austroalpine nappes). The related zircon fission track data are mostly >100 My old with a small, younger, but badly constrained age peak of 41 ± 9 My (Spiegel et al., 2000). This would favor a dominant input from the Austroalpine nappes, which yield cooling ages older than ca. 50 My (e.g. Bernet et al., 2009; Gemignani et al. 2017), rather than from the Lepontine nappes, which is characterized by zircon fission track ages younger than ca. 30 My (e.g. Hurford, 1986). During this time, the drainage divide is probably located close to the Insubric line (e.g. Schlunegger et al., 1998), but north of the Bergell pluton (Fig. 8a), whose detritus is exclusively found in the retroforeland in the south (Gonfolite Lombarda, Giger and Hurford, 1989; Carrapa and Di Giulio, 2001).

Garnets in the 19 My old Molasse indicate a mixed contribution of sources that could be located in the Lepontine nappes as well as the Prealps Romandes (Fig. 8b). This is supported by the related young (<30 My) zircon fission track ages (Spiegel et al. 2000) and the abundant flysch pebbles (Schlunegger et al., 1998), respectively. A potential contribution from ophiolites, as suggested by Spiegel et al. (2002), could be supported by the few eclogite facies garnet grains found in the 19 My old sample. Their source could be located in the Penninic nappes in the hanging wall of the Rhone-Simplon line or in the Penninic nappes located between the Lepontine and the Austroalpine nappes (Fig. 8b). The Lepontine dome was probably drained both towards the north and the south (Fig. 8b), because old basement detritus with young cooling ages (~30 My, derived from K/Ar on white mica) was found in the Gonfolite Lombarda group in the southern retroforeland (Giger and Hurford, 1989).

Finally, the garnet data suggests a dominant contribution from the external massifs and/or the Gotthard nappe at around 14 My ago (Fig. 8c). We suggest that the drainage divide was essentially located at its current position (Fig. 8c, d), but this warrants corroboration from other deposits in the foreland and the retroforeland.

5. Conclusions

Garnet geochemistry is a useful tool to further constrain the provenance of ~~sediments~~ sandstones in orogens such as the Central Alps. We have demonstrated that it is possible to distinguish detrital garnets using a combination of garnet classification schemes (Mange and Morton, 2007; Tolosana-Delgado et al., 2018) and case-specific comparison with available Alpine source rock compositions (Stutenbecker et al., 2017). For the Miocene deposits of the Swiss Molasse basin, we were able to (1) confirm the provenance shift possibly related to the exhumation of the Lepontine dome between 25 and 19 My ago as suggested by previous studies (e.g.: von Eynatten, 2003) and (2) to identify an

additional provenance shift between ca. 19 and 14 My ago that had not been noticed before. ~~The-This latter shift before 14 My ago shift~~ is related to the erosion of granites from the external crystalline massifs, which provides a minimum age for their surficial exposure and corroborates their recently revised structural geometry. ~~(Fig. 7b). We conclude that the exposure of the crystalline basement happened already ca. 14 My ago, which is several million years earlier than previously assumed. In contrast to most previous studies, conclude that parts of the crystalline basement must have been exposed already ca. 14 My ago.~~

Author contribution

LS designed the project. AM helped during field work and sample collection. PT and PL gave advice for sample preparation, supported the microprobe measurements and data acquisition at the University of Bern. LS prepared the manuscript with contributions by all co-authors.

Acknowledgements

This project was financially supported by a post-doctoral research grant awarded to L. Stutenbecker by the International Association of Sedimentologists (IAS). We would like to thank Fritz Schlunegger for guidance in the field and Alfons Berger and Lukas Nibourel for stimulating discussions. We thank reviewers Carita Augustsson and Lorenzo Gemignani for their constructive comments.

References

- Allen, P.A., Crampton, S. L. and Sinclair, H.D.: The inception and early evolution of the North Alpine Foreland Basin, Switzerland. Basin Res., 3, 143-163, 1991.
- Andò, S., Morton, A.C., and Garzanti, E.: Metamorphic grade of source rocks revealed by chemical fingerprints of detrital amphibole and garnet. Geol. Soc. Spec. Publ., 386, 351–371, doi:10.1144/SP386.5, 2014.
- Angiboust, S., Agard, P., Jolivet, L., and Beyssac, O.: The Zermatt-Saas ophiolite: The largest (60-km wide) and deepest (c. 70-80km) continuous slice of oceanic lithosphere detached from a subduction zone? Terra Nova, 21, 171–180, doi:10.1111/j.1365-3121.2009.00870.x, 2009.
- Armstrong, J.T.: Quantitative analysis of silicate and oxide minerals: a reevaluation of ZAF corrections and proposal for new Bence–Albee coefficients, in: Microbeam Analysis, edited by Romig, A.D. and Goldstein, J.I., San Francisco Press, USA, 208–212, 1984.
- Baran, R., Friedrich, A.M., and Schlunegger, F.: The late Miocene to Holocene erosion pattern of the Alpine foreland basin reflects Eurasian slab unloading beneath the western Alps rather than global climate change. Lithosphere, 6, 124–131, doi:10.1130/L307.1, 2014.
- Berger, A., Mercolli, I., and Engi, M.: The central Lepontine Alps: Notes accompanying the tectonic and petrographic map sheet Sopra Ceneri (1:100'000). Schweiz. Miner. Petrog., 85, 109–146, 2005.
- Bernet, M., Brandon, M., Garver, J., Balestieri, M.L., Ventura, B., and Zattin, M.: Exhuming the Alps through time: clues from detrital zircon fission-track thermochronology. Basin Res., 21, 781-798, doi: 10.1111/j.1365-2117.2009.00400.x, 2009.
- Bousquet, R., Oberhänsli, R., Schmid, S.M., Berger, A., Wiederkehr, M., Robert, C., Möller, A., Rosenberg, C., Zeilinger, G., Molli, G., and Koller, F.: Metamorphic Framework of the Alps. Commission for the geological map of the world, Paris, 2012.
- Bucher, S., and Bousquet, R.: Metamorphic evolution of the Briançonnais units along the ECORS-

- 577 CROP profile (Western Alps): New data on metasedimentary rocks. *Swiss J. Geosci.*, 100, 227–242,
578 doi:10.1007/s00015-007-1222-4, 2007.
- 579 Bucher, K., and Grapes, R.: The eclogite-facies Allalin gabbro of the Zermatt-Saas ophiolite, Western
580 alps: A record of subduction zone hydration. *J. Petrol.*, 50, 1405–1442, doi:10.1093/petrology/egp035,
581 2009.
- 582 Carrapa, B., and Di Giulio, A.: The sedimentary record of the exhumation of a granitic intrusion into a
583 collisional setting: The lower Gonfolite Group, Southern Alps, Italy. *Sedimentary Geol.*, 139, 217-
584 228, 2001.
- 585 Cartwright, I., and Barnicoat, A.C.: Petrology, geochronology, and tectonics of shear zones in the
586 Zermatt-Saas and Combin zones of the Western Alps. *J. Metamorph. Geol.*, 20, 263–281, 2002.
- 587 Cederbom, C.E., Sinclair, H.D., Schlunegger, F., and Rahn, M.K.: Climate-induced rebound and
588 exhumation of the European Alps. *Geology*, 32, 709-712, doi: 10.1130/G20491.1, 2004.
- 589 Cenki-Tok, B., Darling, J.R., Rolland, Y., Dhuime, B., and Storey, C.D.: Direct dating of mid-crustal
590 shear zones with synkinematic allanite: New in situ U-Th-Pb geochronological approaches applied to
591 the Mont Blanc massif. *Terra Nova*, 26, 29–37, doi:10.1111/ter.12066, 2014.
- 592 Challandes, N., Marquer, D., and Villa, I.M.: P-T-t modelling, fluid circulation, and ³⁹Ar-⁴⁰Ar and
593 Rb-Sr mica ages in the Aar Massif shear zones (Swiss Alps). *Swiss J. Geosci.*, 101, 269–288,
594 doi:10.1007/s00015-008-1260-6, 2008.
- 595 Champagnac, J.-D., Schlunegger, F., Norton, K., von Blanckenburg, F., Abbühl, L.M., and Schwab,
596 M.: Erosion-driven uplift of the modern Central Alps. *Tectonophysics*, 474, 236-249, doi:
597 10.1016/j.tecto.2009.02.024, 2009.
- 598 Chinner, G.A., and Dixon, J.E.: Some high-pressure parageneses of the allalin gabbro, Valais,
599 Switzerland. *J. Petrol.*, 14, 185–202, doi:10.1093/petrology/14.2.185, 1973.
- 600 Deer, W., Howie, R.A., and Zussmann, J.: An introduction to the rock-forming minerals. New Jersey:
601 Prentice Hall, 1992.
- 602 Engesser, B.: Die Eomyidae (Rodentia, Mammalia) der Molasse der Schweiz und Savoyens.
603 Systematik und Biostratigraphie. Schweizer Paläontologische Abhandlungen (112), Basel: Birkhäuser
604 Verlag, 1990.
- 605 Engi, M., Giuntoli, F., Lanari, P., Burn, M., Kunz, B., and Bouvier, A.S.: Pervasive Eclogitization Due
606 to Brittle Deformation and Rehydration of Subducted Basement: Effects on Continental Recycling?
607 *Geochem. Geophys. Geosy.*, 19, 865–881, doi:10.1002/2017GC007215, 2018.
- 608 Ernst, W.G., and Dal Piaz, G. V.: Mineral parageneses of eclogitic rocks and related mafic schists of
609 the Piemonte ophiolite nappe, Breuil-St Jacques area, Italian Western Alps. *Amer. Mineral.*, 63, 621–
610 640, 1978.
- 611 ~~von Eynatten, H.: Petrography and chemistry of sandstones from the Swiss Molasse Basin: An archive~~
612 ~~of the Oligocene to Miocene evolution of the Central Alps. *Sedimentology*, 50, 703–724,~~
613 ~~doi:10.1046/j.1365-3091.2003.00571.x, 2003.~~
- 614 ~~von Eynatten, H., and Wijbrans, J.R.: Precise tracing of exhumation and provenance using ⁴⁰Ar/³⁹Ar~~
615 ~~geochronology of detrital white mica: the example of the Central Alps. *Geol. Soc. Spec. Publ.*, 208,~~
616 ~~289–305, 2003.~~
- 617 Fox, M., Herman, F., Kissling, E., and Willett, S.D.: Rapid exhumation in the Western Alps driven by
618 slab detachment and glacial erosion. *Geology*, 43, 379–382, doi:10.1130/G36411.1, 2015.
- 619 Frey, M., Desmons, J., and Neubauer, F.: The new metamorphic map of the Alps: introduction.

Schweiz. Miner. Petrog., 79, 1–4, doi:10.5169/seals-60194, 1999.

Frey, M., and Ferreiro Mählmann, R.: Alpine metamorphism of the Central Alps. Schweiz. Miner. Petrog., 79, 135–154, 1999.

Froitzheim, N., Schmid, S.M., and Frey, M.: Mesozoic paleogeography and the timing of eclogite facies in the Alps: A working hypothesis. Eclogae Geol. Helv., 110, 81–110, 1996.

Garzanti, E., and Andò, S.: Plate Tectonics and Heavy Mineral Suites of Modern Sands-, in: [Heavy minerals in use, edited by Mange, M.A. and Wright, D.T.](#), Developments in Sedimentology [series](#), 58, 741–763, doi:10.1016/S0070-4571(07)58029-5, 2007.

Gebauer, D.: Alpine geochronology of the Central and Western Alps: new constraints for a complex geodynamic evolution. Schweiz. Miner. Petrog., 79, 191–208, doi:10.5169/seals-60205, 1999.

[Giger, M., and Hurford, A.J.: Tertiary intrusives of the Central Alps: Their Tertiary uplift, erosion, redeposition and burial in the south-alpine foreland. Eclogae Geol. Helv., 82, 857–866, 1989.](#)

Giuntoli, F., Lanari, P., and Engi, M.: Deeply subducted continental fragments - Part 1: Fracturing, dissolution-precipitation, and diffusion processes recorded by garnet textures of the central Sesia Zone (western Italian Alps). Solid Earth, 9, 167–189, doi:10.5194/se-9-167-2018, 2018.

Glotzbach, C., Reinecker, J., Danišik, M., Rahn, M., Frisch, W., and Spiegel, C.: Thermal history of the central Gotthard and Aar massifs, European Alps: Evidence for steady state, long-term exhumation: J. Geophys. Res. - Earth, 115, doi:10.1029/2009JF001304, 2010.

Handy, M.R., Schmid, S., Bousquet, R., Kissling, E., and Bernoulli, D.: Reconciling plate-tectonic reconstructions of Alpine Tethys with the geological-geophysical record of spreading and subduction in the Alps. Earth-Sci. Rev., 102, 121–158, doi:10.1016/j.earscirev.2010.06.002, 2010.

[Herman, F., Seward, D., Valla, P.G., Carter, A., Kohn, B., Willett, S.D., and Ehlers, T.A.: Worldwide acceleration of mountain erosion under a cooling climate. Nature, 504, 423–426, doi: 10.1038/nature12877, 2013.](#)

Herwegh, M., Berger, A., Baumberger, R., Wehrens, P., and Kissling, E.: Large-Scale Crustal-Block-Extrusion During Late Alpine Collision. Sci. Rep., 7, 413, doi:10.1038/s41598-017-00440-0, 2017.

Hunziker, J.C., and Zingg, A.: Lower palaeozoic amphibolite to granulite facies metamorphism in the Ivrea zone (Southern Alps, Northern Italy). Schweiz. Miner. Petrog., 60, 181–213, 1980.

Hurford, A.J.: Cooling and uplift patterns in the Lepontine Alps South Central Switzerland and an age of vertical movement on the Insubric fault line. Contrib. Mineral. Petr., 92, 413–427, doi:10.1007/BF00374424, 1986.

[Ingersoll, R.V.: Actualistic sandstone petrofacies: Discriminating modern and ancient source rocks. Geology, 18, 733–736, 1990.](#)

Janots, E., Engi, M., Rubatto, D., Berger, A., Gregory, C., and Rahn, M.: Metamorphic rates in collisional orogeny from in situ allanite and monazite dating. Geology, 37, 11–14, doi:10.1130/G25192A.1, 2009.

Kempf, O., Matter, A., Burbank, D.W., and Mange, M.: Depositional and structural evolution of a foreland basin margin in a magnetostratigraphic framework: The eastern Swiss Molasse Basin. Int. J. Earth Sci., 88, 253–275, doi:10.1007/s005310050263, 1999.

Krippner, A., Meinhold, G., Morton, A.C., and von Eynatten, H.: Evaluation of garnet discrimination diagrams using geochemical data of garnets derived from various host rocks. Sedimentary Geol., 306, 36–52, doi:10.1016/j.sedgeo.2014.03.004, 2014.

- Kuhlemann, J., and Kempf, O.: Post-Eocene evolution of the North Alpine Foreland Basin and its response to Alpine tectonics. *Sedimentary Geol.*, 152, 45–78, doi:10.1016/S0037-0738(01)00285-8, 2002.
- Kuhlemann, J., Frisch, W., Székely, B., Dunkl, I., and Kázmér, M.: Post-collisional sediment budget history of the Alps: tectonic versus climatic control. *Int. J. Earth Sci.*, 91, 818-837, doi: 10.1007/s00531-002-0266-y, 2002.
- Kühni, A., and Pfiffner, O.A.: The relief of the Swiss Alps and adjacent areas and its relation to lithology and structure: Topographic analysis from a 250-m DEM. *Geomorphology*, 41, 285–307, doi:10.1016/S0169-555X(01)00060-5, ~~2000~~2001.
- Locock, A.J.: An Excel spreadsheet to recast analyses of garnet into end-member components, and a synopsis of the crystal chemistry of natural silicate garnets. *Comput. Geosci.*, 34, 1769–1780, doi:10.1016/j.cageo.2007.12.013, 2008.
- Malusà, M., Resentini, A., and Garzanti, E.: Hydraulic sorting and mineral fertility bias in detrital geochronology. *Gondwana Research.*, 31, 1-19, doi:10.1016/j.gr.2015.09.002, 2016.
- ~~Mange, M.A., and Morton, A.C.: Geochemistry of heavy minerals–, in: Heavy minerals in use, edited by Mange, M.A. and Wright, D.T.,~~ Developments in Sedimentology series, 58, 345–391, 2007.
- Matter, A.: Sedimentologische Untersuchungen im östlichen Napfgebiet (Entlebuch - Tal der Grossen Fontanne, Kt. Luzern). *Eclogae Geol. Helv.*, 57, 315–428, 1964.
- Michalski, I., and Soom, M.: The Alpine thermo-tectonic evolution of the Aar and Gotthard massifs, Central Switzerland - Fission Track ages on zircon and apatite and K-Ar mica ages. *Schweiz. Miner. Petrog.*, 70, 373–387, doi:10.5169/seals-53628, 1990.
- ~~Morton, A.C., and Hallsworth, C.: Stability of Detrital Heavy Minerals During Burial Diagenesis, in: Heavy minerals in use, edited by Mange, M.A. and Wright, D.T.,~~–Developments in Sedimentology series, 58, 215–245, doi:10.1016/S0070-4571(07)58007-6, 2007.
- Nibourel, L., Berger, A., Egli, D., Luensdorf, N.K., and Herwegh, M.: Large vertical displacements of a crystalline massif recorded by Raman thermometry. *Geology*, 46, 879–882, doi:10.1130/G45121.1, 2018.
- Oberhänsli, R.: P-T Bestimmungen anhand von Mineralanalysen in Eklogiten und Glaukophaniten der Ophiolite von Zermatt. *Schweiz. Miner. Petrog.*, 60, 215–235, doi:10.5169/seals-46668, 1980.
- Oberhänsli, R., Bousquet, R., Engi, M., Goffé, B., Gosso, G., Handy, M.R., Höck, V., Koller, F., Lardeaux, J.M., Polino, R., Rossi, P.L., Schuster, R., Schwartz, S., Spalla, I.: Metamorphic Structure of the Alps. CCGM Commission of the Geological Maps of the World, 2004.
- Pfiffner, O.A.: Evolution of the north Alpine foreland basin in the Central Alps, in: Foreland basins, edited by Allen, P.A. and Homewood, P., *Int. As. Sed.*, 8, 219–228, 1986.
- Pfiffner, O.A.: Thick-Skinned and Thin-Skinned Tectonics: A Global Perspective. *Geosciences*, 7, 71, doi:10.3390/geosciences7030071, 2017.
- Pfiffner, O.A., Schlunegger, F., and Buiter, S.J.H.: The Swiss Alps and their peripheral foreland basin: Stratigraphic response to deep crustal processes. *Tectonics*, 21, 3.1-3.16, doi:10.1029/2000TC900039, 2002.
- Ragusa, J., Kindler, P., Šegvić, B., and Ospina-Ostios, L.M.: Provenance analysis of the Voirons Flysch (Gurnigel nappe, Haute-Savoie, France): stratigraphic and palaeogeographic implications. *Springer Berlin Heidelberg*, 106, 2619-2651, doi:10.1007/s00531-017-1474-9, 2017.
- von Raumer, J.F., Abrecht, J., Bussy, F., Lombardo, B., Menot, R.-P., and Schaltegger, U.: The

705 Palaeozoic metamorphic evolution of the Alpine External Massifs. *Schweiz. Miner. Petrog.*, 79, 5–22,
706 1999.

707 Reinecke, T.: Prograde high- to ultrahigh-pressure metamorphism and exhumation of oceanic
708 sediments at Lago di Cignana, Zermatt-Saas Zone, western Alps. *Lithos*, 42, 147–189,
709 doi:10.1016/S0024-4937(97)00041-8, 1998.

710 Rolland, Y., Rossi, M., Cox, S.F., Corsini, M., Mancktelow, N., Pennacchioni, G., Fornari, M., and
711 Boullier, A.M.: 40Ar/39Ar dating of synkinematic white mica: insights from fluid-rock reaction in
712 low-grade shear zones (Mont Blanc Massif) and constraints on timing of deformation in the NW
713 external Alps. *Geol. Soc. Spec. Publ.*, 299, 293–315, doi:10.1144/SP299.18, 2008.

714 Sartori, M.: L'unité du Barrhorn (Zone pennique, Valais, Suisse). *Mémoires de Géologie* 6, Lausanne,
715 Switzerland, 1990.

716 Sartori, M., Gouffon, Y., and Marthaler, M.: Harmonisation et définition des unités
717 lithostratigraphiques briançonnaises dans les nappes penniques du Valais. *Eclogae Geol. Helv.*, 99,
718 363–407, doi:10.1007/s00015-006-1200-2, 2006.

719 Schaer, J. P., Reimer, G.M., and Wagner, G.A.: Actual and ancient uplift rate in the Gotthard region,
720 Swiss Alps: A comparison between precise levelling and Fission-Track Apatite age. *Tectonophysics*,
721 29, 293–300, doi:10.1016/0040-1951(75)90154-7, 1975.

722

723 [Schildgen, T.F., van der Beek, P.A., Sinclair, H.D., and Thiede, R.C.: Spatial correlation bias in late-](#)
724 [Cenozoic erosion histories derived from thermochronology. *Nature*, 559, 89-93, doi: 10.1038/s41586-](#)
725 [018-0260-6, 2018.](#)

726 Schlunegger, F., Burbank, D.W., Matter, A., Engesser, B., and Mödden, C.: Magnetostratigraphic
727 calibration of the Oligocene to Middle Miocene (30-15 Ma) mammal biozones and depositional
728 sequences of the Swiss Molasse Basin. *Eclogae Geol. Helv.*, 89, 753–788, 1996.

729 Schlunegger, F., and Kissling, E.: Slab rollback orogeny in the Alps and evolution of the Swiss
730 Molasse basin. *Nat. Commun.*, 6, 1-10, 8605, doi:10.1038/ncomms9605, 2015.

731 Schlunegger, F., Matter, A., and Mange, M.A.: Alluvial-Fan Sedimentation and Structure of the
732 Southern Molasse Basin Margin, Lake Thun Area, Switzerland. *Eclogae Geol. Helv.*, 86, 717–750,
733 1993.

734 Schlunegger, F., Slingerland, R., and Matter, A.: Crustal thickening and crustal extension as controls
735 on the evolution of the drainage network of the central Swiss Alps between 30 Ma and the present:
736 Constraints from the stratigraphy of the North Alpine Foreland Basin and the structural evolution of
737 the Basin. *Basin Res.*, 10, 197–212, doi:10.1046/j.1365-2117.1998.00063.x, 1998.

738 Schmid, S.M., Fügenschuh, B., Kissling, E., and Schuster, R.: Tectonic map and overall architecture
739 of the Alpine orogen. *Eclogae Geol. Helv.*, 97, 93–117, doi:10.1007/s00015-004-1113-x, 2004.

740 Schmid, S.M., Pfiffner, O.A., Froitzheim, N., Schönborn, G., and Kissling, E.: Geophysical -
741 geological transect and tectonic evolution of the Swiss-Italian Alps. *Tectonics*, 15, 1036–1064,
742 doi:10.1029/96TC00433, 1996.

743 Sinclair, H.D., Coakley, B.J., Allen, P.A., and Watts, A.B.: Simulation of foreland basin stratigraphy
744 using a diffusion model of mountain belt uplift and erosion: An example from the Central Alps,
745 Switzerland. *Tectonics*, 10, 599–620, 1991.

746 [Sinclair, H.D.: Flysch to molasse transition in peripheral foreland basins: The role of the passive](#)
747 [margin versus slab breakoff. *Geology*, 25, 1123-1126, 1997.](#)

748 Spear, F.S.: *Metamorphic Phase Equilibria And Pressure-Temperature-Time-Paths* (2nd ed.)

749 Mineralogical Society of America monograph, USA, 1994.

750 Spiegel, C., Kuhlemann, J., Dunkl, I., Frisch, W., Von Eynatten, H., and Balogh, K.: The erosion
751 history of the Central Alps: Evidence from zircon fission track data of the foreland basin sediments.
752 *Terra Nova*, 12, 163–170, doi:10.1046/j.1365-3121.2000.00289.x, 2000.

753 Spiegel, C., Siebel, W., Frisch, W., and Berner, Z.: Nd and Sr isotopic ratios and trace element
754 geochemistry of epidote from the Swiss Molasse Basin as provenance indicators: Implications for the
755 reconstruction of the exhumation history of the Central Alps. *Chem. Geol.*, 189, 231–250,
756 doi:10.1016/S0009-2541(02)00132-8, 2002.

757 Spillmann, P.: Die Geologie des Grenzbereichs im penninisch-ostalpinen südlichen Berninagebirge,
758 Ph.D. thesis, ETH Zürich, Switzerland, 262pp., 1993.

759 Spillmann, P., and Büchi, H.: The Pre-Alpine Basement of the Lower Austro-Alpine Nappes in the
760 Bernina Massif (Grisons, Switzerland; Valtellina, Italy), in: *The Pre-Mesozoic Geology in the Alps*,
761 edited by von Raumer, J.F. and Neubauer, F., Springer Berlin Heidelberg, Germany, 457–467, 1993.

762 Steck, A., and Burri, G.: Chemismus und Paragenesen von Granaten aus Granitgneisen der
763 Grünschiefer- und Amphibolitfazies der Zentralalpen. *Schweiz. Miner. Petrog.*, 51, 534–538, 1971.

764 Stutenbecker, L., Delunel, R., Schlunegger, F., Silva, T.A., Šegvić, B., Girardclos, S., Bakker, M.,
765 Costa, A., Lane, S.N., Loizeau, J.-L., Molnar, P., Akçar, N. and Christl, M.: Reduced sediment supply
766 in a fast eroding landscape? A multi-proxy sediment budget of the upper Rhône basin, Central Alps.
767 *Sedimentary Geol.*, 375, 105–119, doi:10.1016/j.sedgeo.2017.12.013, 2018.

768 Stutenbecker, L., Berger, A., and Schlunegger, F.: The potential of detrital garnet as a provenance
769 proxy in the Central Swiss Alps. *Sedimentary Geol.*, 351, 11–20, doi:10.1016/j.sedgeo.2017.02.002,
770 2017.

771 Stutenbecker, L., 2019, Detrital garnet chemistry from the Molasse basin ([supplementary data](#)). doi:
772 10.6084/m9.figshare.8269742.v1.

773 Thélin, P., Sartori, M., Lengeler, R., and Schaerer, J.-P.: Eclogites of Paleozoic or early Alpine age in
774 the basement of the Penninic Siviez-Mischabel nappe, Wallis, Switzerland. *Lithos*, 25, 71–88, 1990.

775 Tolosana-Delgado, R., von Eynatten, H., Krippner, A., and Meinhold, G.: A multivariate
776 discrimination scheme of detrital garnet chemistry for use in sedimentary provenance analysis.
777 *Sedimentary Geol.*, 375, 14–26, doi:10.1016/j.sedgeo.2017.11.003, 2018.

778 Trümpy, R.: *Geology of Switzerland. A guide book, Part A: An outline of the geology of Switzerland*.
779 Basel, Switzerland: Wepf, 1980.

780 Vernon, A.J., van der Beek, P.A., and Sinclair, H.D.: Spatial correlation between long-term
781 exhumation rates and present-day forcing parameters in the western European Alps. *Geology*, 37, 859–
782 862, doi:10.1130/G25740A.1, 2009.

783 Vernon, A.J., van der Beek, P.A., Sinclair, H.D., and Rahn, M.K.: Increase in late Neogene denudation
784 of the European Alps confirmed by analysis of a fission-track thermochronology database. *Earth*
785 *Planet. Sc. Lett.*, 270, 316–329, doi:10.1016/j.epsl.2008.03.053, 2008.

786 [von Eynatten, H.: Petrography and chemistry of sandstones from the Swiss Molasse Basin: An archive](#)
787 [of the Oligocene to Miocene evolution of the Central Alps. *Sedimentology*, 50, 703–724,](#)
788 [doi:10.1046/j.1365-3091.2003.00571.x, 2003.](#)

789 [von Eynatten, H., and Wijbrans, J.R.: Precise tracing of exhumation and provenance using \$^{40}\text{Ar}/^{39}\text{Ar}\$](#)
790 [geochronology of detrital white mica: the example of the Central Alps. *Geol. Soc. Spec. Publ.*, 208,](#)
791 [289–305, 2003.](#)

792 Wagner, G. A., Reimer, G.M., and Jäger, E.: Cooling ages derived by apatite fission track, mica Rb-Sr
793 and K-Ar dating: The uplift and cooling history of the central Alps, *Memorie degli Istituti di Geologia*
794 *e Mineralogia dell' Università di Padova*, 30, 1-27, 1977.

795

796 Weber, S., and Bucher, K.: An eclogite-bearing continental tectonic slice in the Zermatt–Saas high-
797 pressure ophiolites at Trockener Steg (Zermatt, Swiss Western Alps). *Lithos*, 232, 336–359,
798 doi:10.1016/j.lithos.2015.07.010, 2015.

799 Wildi, W.: Heavy mineral distribution and dispersal pattern in penninic and ligurian flysch basins
800 (Alps, northern Appennines). *Giorn. Geol.*, 47, 77–99, 1985.

801 Winkler, W.: The tecto-metamorphic evolution of the Cretaceous northern Adriatic margin as recorded
802 by sedimentary series (western part of the Eastern Alps). *Eclogae Geol. Helv.*, 89, 527-551, 1996.

803 Wittmann, H., von Blanckenburg, F., Kruesmann, T., Norton, K.P., and Kubik, P.W.: Relation
804 between rock uplift and denudation from cosmogenic nuclides in river sediment in the Central Alps of
805 Switzerland. *J. Geophys. Res. - Earth*, 112, F04010, 1–20, doi:10.1029/2006JF000729, 2007.

Table 1: Sample locations and characteristics of the Molasse sandstones from the Honegg-Napf fan.
Abbreviations used: UFM = Upper Freshwater Molasse, UMM = Upper ~~m~~arine Molasse, LFM
= ~~L~~ower Freshwater Molasse.

Sample name	Sampling location	Lithostratigraphy (Matter, 1964; Schlunegger et al. 1996)	Magnetostratigraphic section (Schlunegger et al. 1996)	Magnetostratigraphic age (Schlunegger et al. 1996)
LS2017-3	47.00566 7.971325	UFM, Napf beds	Fontannen section	ca. 14 Ma My
LS2018-5	46.93913 7.950800	UMM, Luzern formation	Schwändigraben section	ca. 19 Ma My
LS2016-18	46.77463 7.732383	LFM, Thun formation	Prässerebach section	ca. 25 Ma My

809 Table 2: Sample locations and characteristics of potential sources (tributary sampling approach)
810 ~~rocks~~

Sample name	Sampling location	River catchment	Metamorphic grade	Lithological unit
LS2018-12	46.72026 7.24548	Ärgera, ca. 30 km ²	Not metamorphic	Gurnigel flysch (detrital garnets)
LS2018-40	46.39026 8.54124	Valle di Foioi, ca. 3 km ²	Alpine amphibolite-facies	Orthogneiss, Antigorio nappe, Lepontine dome
LS2016-43	46.43955 8.50115	Valletta di Fiorina, ca. 8 km ²	Alpine amphibolite-facies	Paragneiss, Lebendun nappe, Lepontine dome

Table 3: ~~Minimum, maximum and average~~ Average contents (including standard deviation in brackets) of the five common garnet endmembers in the Molasse ~~sediments~~ sandstones, the fluvial samples from the Lepontine gneisses and the Gurnigel flysch (this study) and three potential source rocks from the literature: External crystalline massif granites (Stutenbecker et al., 2017), eclogite facies rocks (Chinner & Dixon, 1973; Ernst & Dal Piaz, 1978; Oberhänsli, 1980; Sartori, 1990; Thélin et al., 1990; Reinecke, 1998; Cartwright & Barnicoat, 2002; Angiboust et al., 2009; Bucher & Grapes, 2009; Weber & Bucher, 2015), and granulite facies rocks (Hunziker & Zingg 1980). For the full dataset we refer to Stutenbecker (2019).

Sample	Almandine (%)	Andradite (%)	Grossular (%)	Pyrope (%)	Spessartine (%)
25 My n=110	70 (12)	2 (5)	9 (7)	9 (5)	9 (8)
19 My n=88	65 (16)	3 (13)	16 (12)	9 (8)	5 (6)
14 My n=77	50 (12)	2 (2)	32 (11)	6 (5)	9 (9)
<u>Valle di Foioi (Antigorio orthogneiss)</u> n=45	<u>67 (10)</u>	<u>1 (1)</u>	<u>11 (12)</u>	<u>10 (6)</u>	<u>10 (10)</u>
<u>Valletta di Fiorina (Lebendun paragneiss)</u> n= 56	<u>64 (5)</u>	<u>0 (1)</u>	<u>22 (4)</u>	<u>8 (3)</u>	<u>5 (3)</u>
<u>Ärgera (Gurnigel flysch)</u> n=	<u>69 (12)</u>	<u>2 (1)</u>	<u>9 (7)</u>	<u>14 (8)</u>	<u>6 (9)</u>
<u>Goneri and Wysswasser rivers (eExternal crystalline massif granites)</u> n=212	<u>34 (16)</u>	<u>0 (0)</u>	<u>35 (14)</u>	<u>4 (5)</u>	<u>21 (10)</u>
Eclogite facies n=147	<u>56 (8)</u>	<u>0 (1)</u>	<u>23 (6)</u>	<u>16 (10)</u>	<u>3 (5)</u>
Granulite facies n=18	<u>67 (8)</u>	<u>0 (0)</u>	<u>4 (1)</u>	<u>25 (10)</u>	<u>4 (4)</u>

819 Table 4: Results from classification following Mange & Morton (2007) and Tolosana-Delgado et al.
820 (2018). Using the linear discriminant method of Tolosana-Delgado et al. (2018) garnets ~~were~~ was
821 attributed to one single class if the probability for that class was ≥ 50 %. Several grains were assigned
822 mixed probabilities with < 50 % per class; these are listed separately below.

	Mange & Morton (2007)				Tolosana-Delgado et al. (2018)		
Types after Mange & Morton (2007)	25 My	19 My	14 My	Classes after Tolosana-Delgado et al. (2018)	25 My	19 My	14 My
Ci-type (high-grade metabasic)		5 %	15 %	Eclogites (Class A)		1 %	
B-type (amphibolite facies)	96 %	84 %	80 %	Amphibolites (Class B)	71 — <u>92</u> %	81 %	78 %
A-type (granulite-facies)	3 %	8 %		Granulites (Class C)		9 %	5.5 %
D-type (metasomatic)	1 %	3 %	5 %	Igneous (Class E)	75 %	3 %	12 %
				Mixed probabilities Classes B-C	1 %	1 %	
				Mixed probabilities Classes A-B-C		5 %	4.5 %

823

824

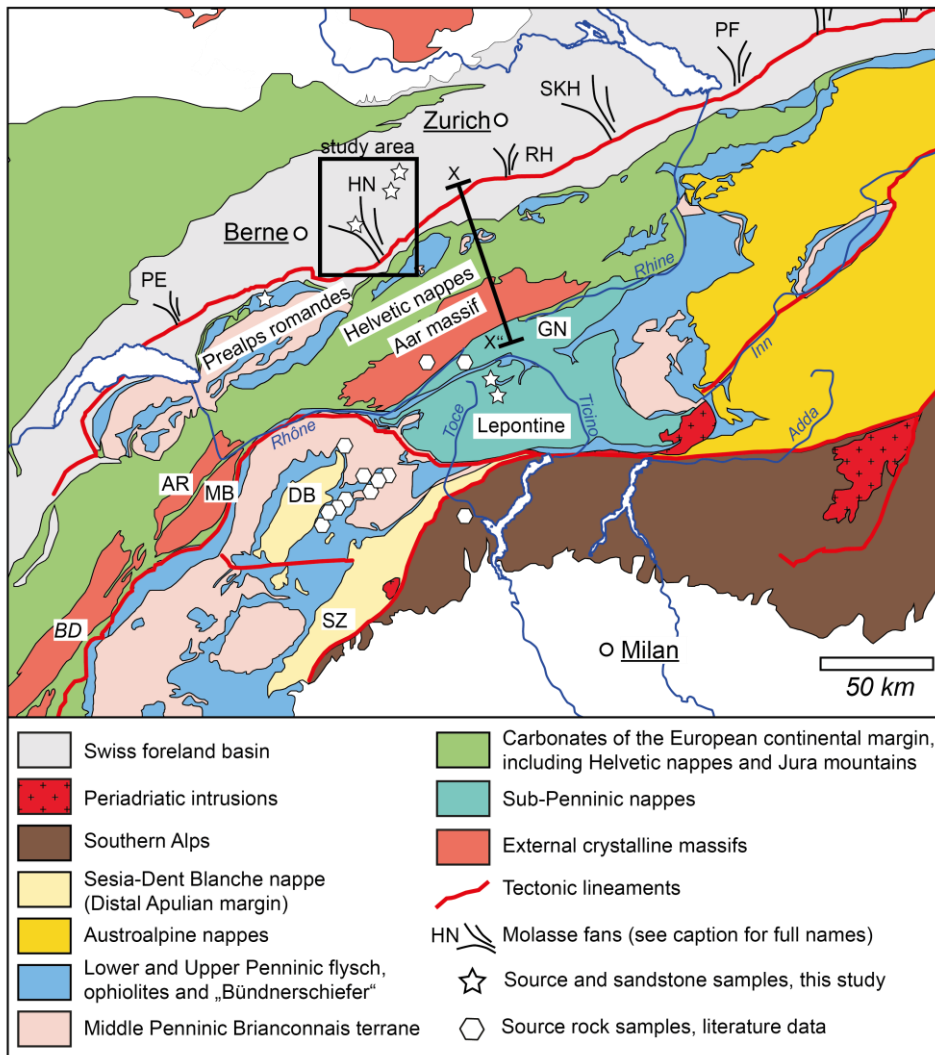


Fig. 1: Simplified tectonic map of the Central Alps after Schmid et al. (2004) highlighting the location of alluvial fan deposits within the northern Alpine foreland basin as well as the most important source rock units in the hinterland. The Honegg-Napf fan, marked by the black rectangle, is located in the central part of the Swiss foreland basin (SFB). For cross section X-X' see Fig. 87. Abbreviations used: AR = Aiguilles-Rouges massif, BD = Belledonne massif, DB = Dent Blanche nappe, HN = Honegg-Napf fan, MB = Mont Blanc massif, GN = Gotthard nappe, PE = Pèlerin fan, PF = Pfänder fan, HN = Honegg-Napf fan, RH = Rigi-Höhronen fan, SKH = Speer-Kronberg-Hörnli fan, SZ = Sesia zone, PF = Pfänder fan.

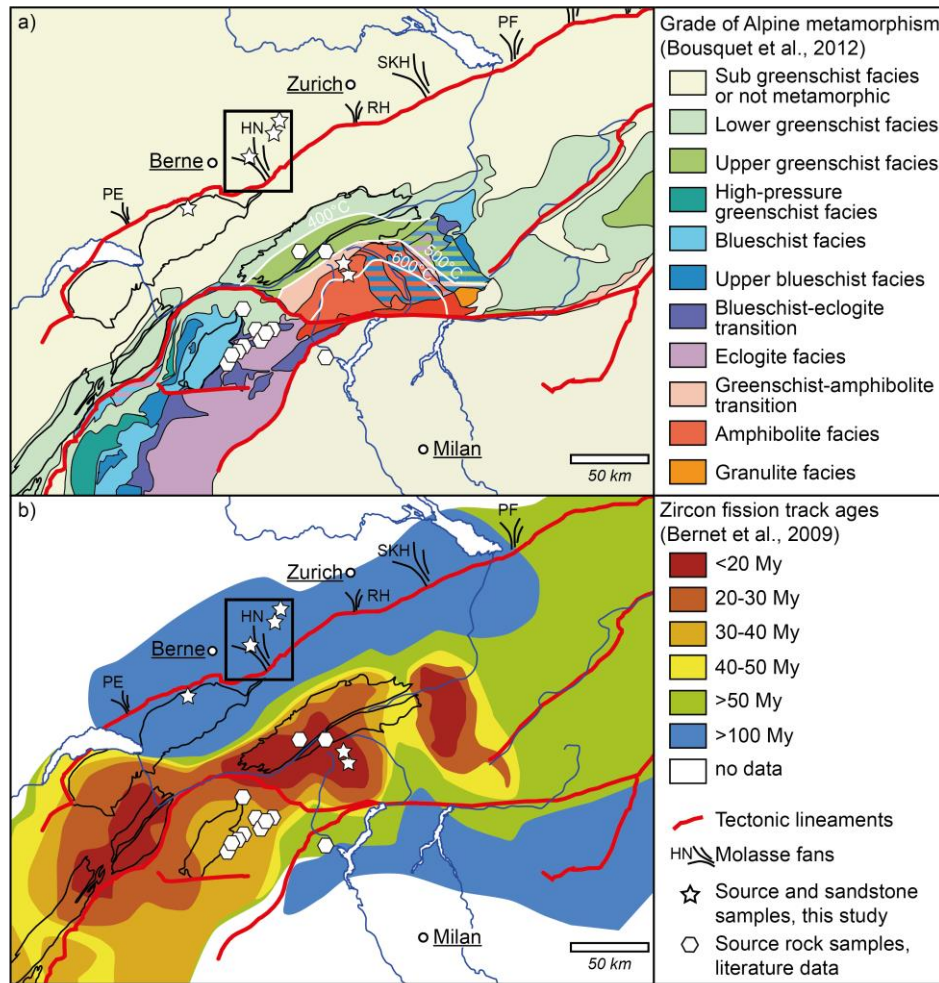


Fig. 2: a) Metamorphic map of the Central Alps (Bousquet et al., 2012) showing the distribution and grade of alpine-Alpine metamorphism. Note the increase from north to south from lower greenschist- to eclogite-facies conditions. b) In-situ bedrock zircon fission track ages according to a compilation of Bernet et al. (2009). Note the predominantly young (<30 My) cooling ages in the area around the Lepontine dome and the external massifs in contrast to the predominantly old (>50 My) cooling ages in the Austroalpine nappes to the east. The river network (blue) and the thick black outlines of selected geological units (external massifs, Prealps Romandes and Dent Blanche nappe, cf. Fig. 1) are used to facilitate the orientation and the comparison with Figure. 1. Abbreviations used: PE = Pèlerin fan, HN = Honegg-Napf fan, RH = Rigi-Höhrnen fan, SKH = Speer-Kronberg-Hörnli fan, PF = Pfänder fan.

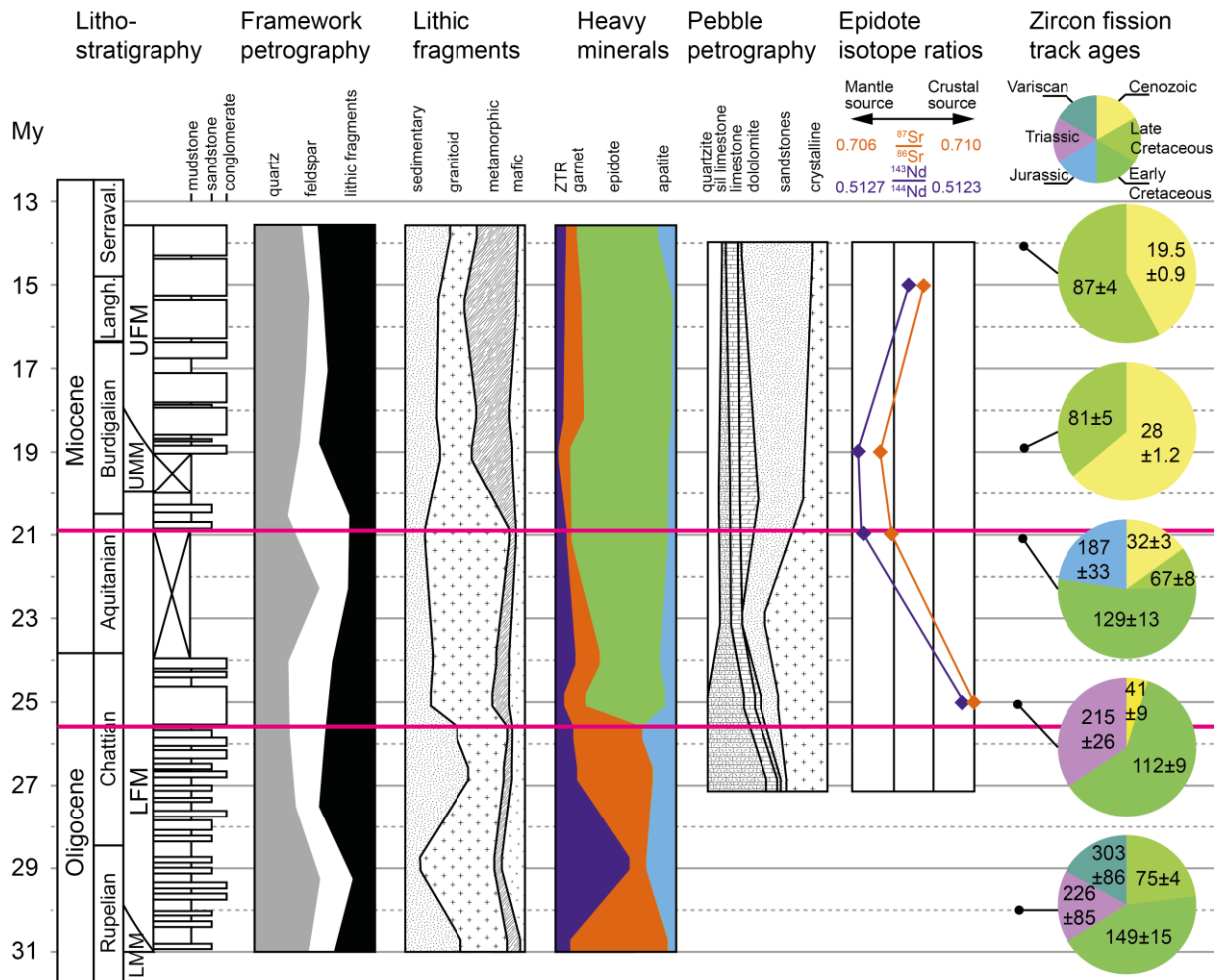


Fig. 3: Compilation of published compositional data in the Honegg-Napf fan. Heavy mineral and rock fragment data from the sand grain size after von Eynatten (2003), pebble petrography after Schlunegger et al. (1998), epidote isotope ratios after Spiegel et al. (2002) and zircon fission-track (FT) data after Spiegel et al. (2000). The two pink lines represent the dominant provenance changes as discussed in the text. Abbreviations used: LMM = Lower Marine Molasse, LFM = Lower Freshwater Molasse, UMM = Upper Marine Molasse, UFM = Upper Freshwater Molasse, ZTR = zircon-tourmaline-rutile-index, sil. = siliceous.

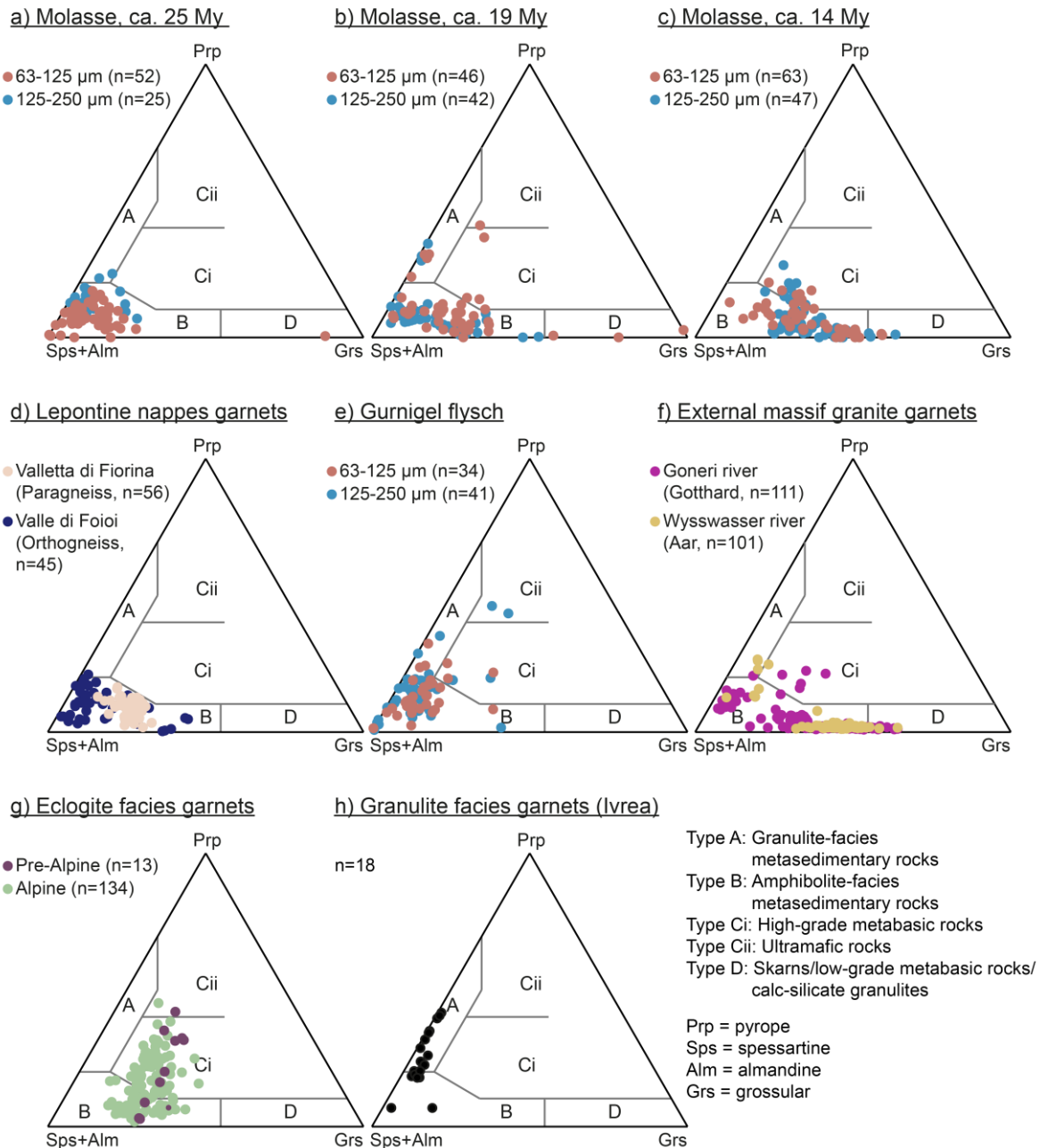


Fig. 4: Ternary plots following Garnet-the- classification scheme of Mange & Morton (2007). (a-c) Detrital garnet compositions in the 25, 19 and 14 My-old Molasse deposits (this study). Garnet provenance changes in Molasse sandstones are marked by an increasing grossular content with decreasing age. Source rock data from (d) Lepontine gneisses (this study), (e) the Gurnigel flysch (this study), (f) external massif granitoids (Stutenbecker et al., 2017), (g) eclogite-facies rocks (Chinner & Dixon, 1973; Ernst & Dal Piaz, 1978; Oberhänsli, 1980; Sartori, 1990; Thélin et al., 1990; Reinecke, 1998; Cartwright & Barnicoat, 2002; Angiboust et al., 2009; Bucher & Grapes, 2009; Weber & Bucher, 2015), (h) granulite-facies rocks from the Ivrea zone in the Southern Alps (Hunziker & Zingg, 1980).

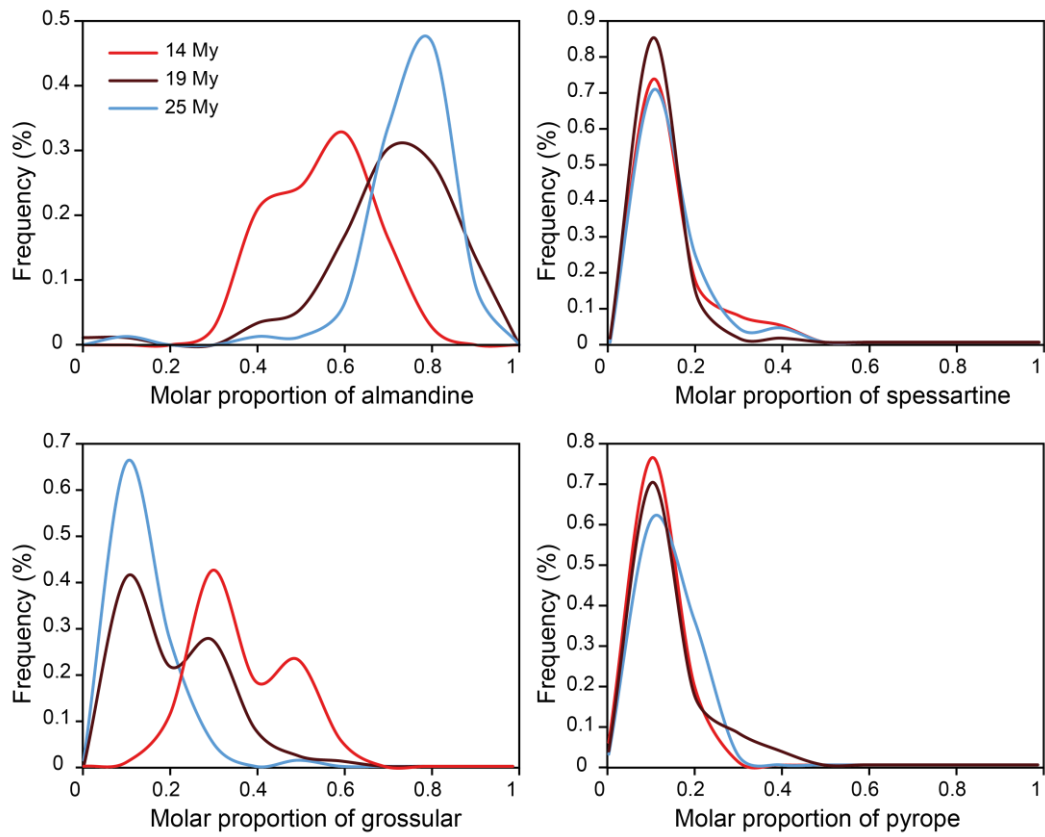


Fig. 5: ~~Shift of garnet compositions between the 25 My, 19 My and 14 My old Molasse samples,~~
~~plotted as r~~Relative frequency of the four most common endmembers almandine, grossular,
spessartine and pyrope in the three detrital samples from the Molasse basin. ~~While spessartine and~~
~~pyrope contents are similar among the three samples, the proportion of almandine decreases and the~~
~~proportion of grossular increases with decreasing age.~~

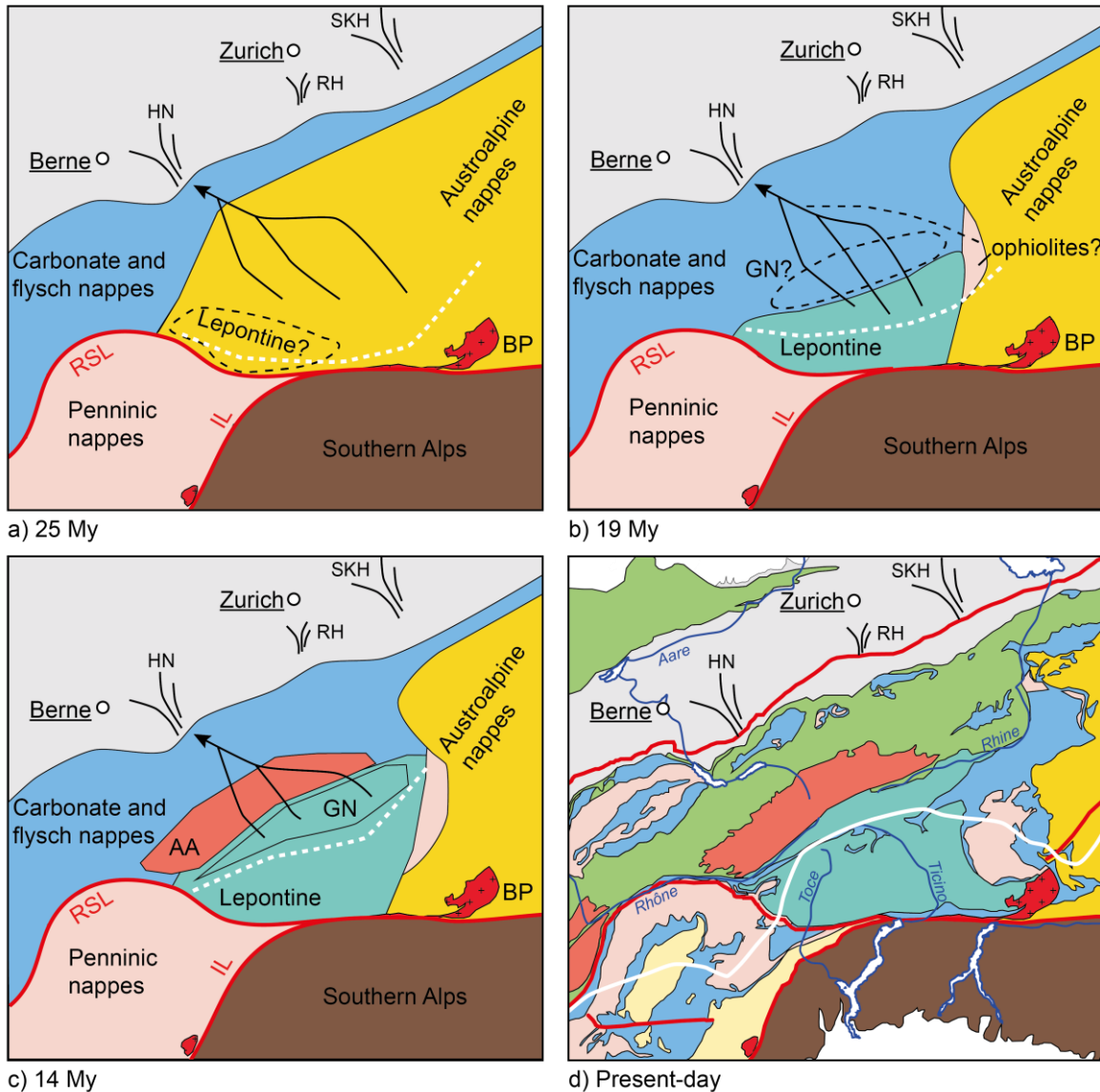
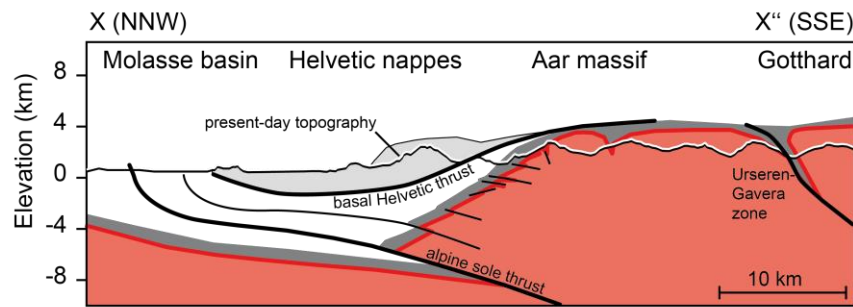


Fig. 76: Paleogeographic reconstruction of the Central Alps, and in particular of the hinterland of the Honegg-Napf fan. Situation during a) the late Oligocene (~25 My), b) the early Miocene (~19 My), c) the middle Miocene (~14 My) and d) today (after Schmid et al., 2004). The color coding in a-c) corresponds essentially to the color coding in d) (—see Fig. 1 for detailed legend). However, we have summarized the lower, middle and upper Penninic nappes and the Dent Blanche nappe (pink color) as well as the carbonate and flysch nappes of the Helvetic nappes and the Prealps Romandes (blue color). —Abbreviations used: AA = Aar massif, BP = Bergell pluton, GN = Gotthard nappe, HN = Honegg-Napf fan, IL = Insubric line, RH = Rigi-Höhrnen fan, RSL = Rhone-Simplon lineament, SKH = Speer-Kronberg-Hörnli fan.

a) Reconstruction after Pfiffner (2017)



b) Reconstruction after Nibourel et al. (2018)

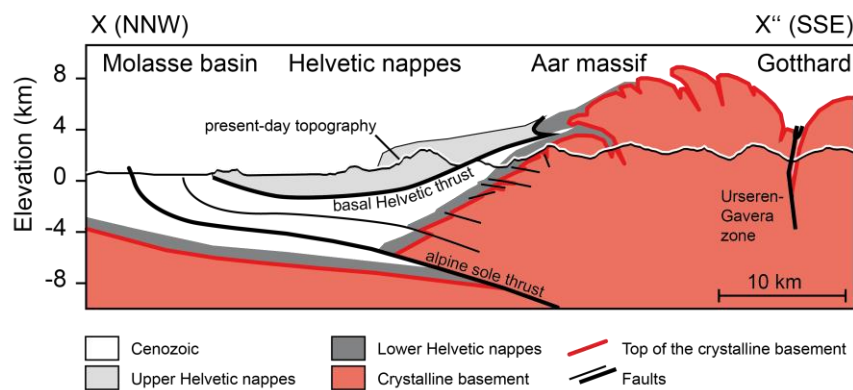


Fig. 7: Cross sections from X to X'' in Figure 1 through the Aar massif simplified after Pfiffner (2017) and Nibourel et al. (2018). ~~For trace of cross section see Fig. 1.~~ (a): The reconstructed top of the crystalline basement in the Aar massif is located ca. 1-2 km higher than the present-day topography according to Pfiffner (2017). (b): In a revised version by Nibourel et al. (2018) the contact between the basement and the overlying Helvetic cover nappes is reconstructed to be steeper, resulting in ca. 8 km of (now eroded) crystalline crust on top of the present-day topography.